Theses and Dissertations

May 2014

A Mathematical Model of Moisture Movement and Bacterial Growth in Two-Dimensional Porous Medium

Rachel Elizabeth TeWinkel
University of Wisconsin-Milwaukee

A MATHEMATICAL MODEL OF MOISTURE MOVEMENT AND BACTERIAL GROWTH IN TWO-DIMENSIONAL POROUS MEDIUM

by

Rachel Elizabeth TeWinkel

A Thesis Submitted in

Partial Fulfillment of the

Requirements for the Degree of

Master of Science

in Mathematics

at

The University of Wisconsin-Milwaukee

May 2014

ABSTRACT
A MATHEMATICAL MODEL OF MOISTURE MOVEMENT AND BACTERIAL GROWTH IN TWO-DIMENSIONAL POROUS MEDIUM

by

Rachel Elizabeth TeWinkel

The University of Wisconsin-Milwaukee, 2014
Under the Supervision of Professor Istvan Lauko

Bacterial growth in sand is of concern in regard to the health of beaches. A mathematical model is presented that represents the movement of moisture and the growth of bacteria through a beach. Simulations were run by numerically solving Richards Equation using a Finite Volume Method in order to track moisture movement. A model of moisture-dependent bacterial growth was then implemented. These simulations show that elevated bacteria counts following rain events do not necessarily result from bacteria in the body of water, but can also be sourced from the sand. Additionally, four different moisture-dependent bacterial growth models are compared to computationally investigate the relationship between relative moisture level in the sand and bacterial growth.

TABLE OF CONTENTS

LIST OF FIGURES

LIST OF TABLES

ACKNOWLEDGMENTS

The author wishes to express her immense gratitude to Dr. Istvan Lauko for his continual support and insight. She also wishes to thank Dr. Gabriella Pinter and Dr. Bruce Wade for their helpful comments.

1   Introduction

The dynamics of bacterial growth in beaches is of concern due to the need to keep public beaches safe for those who frequent them. Certain indicators in the water and sand are monitored in accordance with the standards set by the U.S. Environmental Protection Agency in order to diagnose the health of the beach [38]. Among those indicators are enterococci and *Escherichia coli* [5]. Studies have been done to try to find a good way to predict bacterial growth given factors such as temperature, sunlight, wind patterns, and wave height [15, 37, 39]. Although many researchers are concerned with the level of bacteria in the water, sand has been shown to be a possible source of bacteria contamination and studying this aspect of beach health is currently of interest. While individual factors have been studied, it is difficult to draw conclusions about the impact of each factor given that they each affect bacterial growth in different ways simultaneously and the weather is constantly changing [15, 37].

In this thesis, a brief discussion of the finite volume method is given using an example of a simplified advection equation. We then formulate a finite volume method for Richards Equation in order to model moisture movement in unsaturated conditions in two dimensions with a vertical cross-section of the beach being considered. We implement a bacterial growth model dependent on moisture and nutrient levels. Both mobile and immobile bacteria are considered, where mobile bacteria move through the moisture in the pore space and immobile bacteria are attached to the grains of sand. Since the relationship of the dependence between bacterial growth and moisture is not wholly understood, we explore four growth models with different representations of moisture dependence. We then compare growth when there is no rain on the beach to growth during and after a rain event and end with a brief discussion on the impact of temperature on the growth.

2 Basic Principles of the Finite Volume Method

2.1 Generalized Formulation of a Finite Volume Scheme

The finite volume method involves creating a mesh over the domain and identifying the cell centers. The cells are the subdomain defined by the mesh. The centers are assumed to have an averaged solution to the equation for the entire cell. Meshes used for this method can be structured or unstructured. Common meshes have grids with cells in the shape of polygons [7, 8, 16].

The following shows the process of obtaining the integral form from the differential form of an equation following a generalized example by Causon *et al* [7]. Consider the following two-dimensional linear advection equation over the Cartesian plane:

$$\frac{\partial U}{\partial t} + v_x \frac{\partial U}{\partial x} + v_y \frac{\partial U}{\partial y} = 0, \tag{2.1}$$

where $U = U(x, y, t)$ is a convected concentration and $\langle v_x, v_y \rangle$ is the constant two-dimensional velocity of a medium carrying the concentration. This equation represents uniform flow over time t in the directions of x and y. With the initial condition of $U(x, y, 0) = f(x, y)$, the exact solution of the above equation is $U(x, y, t) = f(x - v_x t, y - v_y t)$ [7]. Equation (2.1) can be written in finite volume form using

$$\vec{H} = U\vec{v},$$

where the flow velocity is $\vec{v} = v_x \vec{i} + v_y \vec{j}$ and $\vec{i}$ and $\vec{j}$ are the Cartesian basis vectors. $\vec{H}$ is a vector field and is referred to as the flux density. Its components measure the rate of mass flow through a unit length [7].

Keeping in mind that ∇ is the differential operator $\vec{i}\frac{\partial}{\partial x} + \vec{j}\frac{\partial}{\partial y}$, (2.1) now becomes:

$$\frac{\partial U}{\partial t} + \nabla \cdot \vec{H} = 0. \tag{2.2}$$

Integrating (2.2) over an arbitrary (simply connected) region D, which can be considered to be an arbitrary volume element, in the Cartesian plane results in [7]:

$$\iint\limits_{D} \left(\frac{\partial U}{\partial t} + \nabla \cdot \vec{H}\right) dD = \iint\limits_{D} 0$$

$$\iint\limits_{D} \frac{\partial U}{\partial t} dD + \iint\limits_{D} \nabla \cdot \vec{H} dD = 0$$

The second term of the above equation can be rewritten using Green's Theorem. A line integral around the perimeter, S, of D gives:

$$\iint\limits_{D} \frac{\partial U}{\partial t} dD + \oint\limits_{S} \vec{H} \cdot \vec{n} ds = 0,$$

where $\vec{n}$ is the outward unit normal vector on S. We then approximate the first integral, resulting in:

$$A\frac{\partial \tilde{U}}{\partial t} + \oint\limits_{S} \vec{H} \cdot \vec{n} ds = 0,$$

where $\tilde{U}$ is the approximate value of U over D, and A is the area of D [7]. Thus, the differential equation can be written in the form:

$$\frac{\partial \tilde{U}}{\partial t} = -\frac{1}{A} \oint\limits_{S} \vec{H} \cdot \vec{n} dS \tag{2.3}$$

This holds for any region over the x-y plane where (2.1) holds. Equation (2.3) is approximated over each volume element, or, cell to produce the finite volume scheme.

Thus, by knowing $\vec{H}$, the length of the sides of each cell, and $\vec{n}$, the normal vector, which is constant on each side, this method can be applied to approximate solutions over the entire grid [7].

Figure 2.1 shows an example of one cell in the mesh grid with normal vectors on two sides.
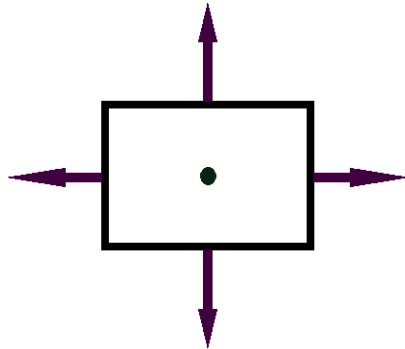
Figure 2.1: A single cell with vectors indicating the outward normal to each of the the cell walls.

3 Finite Volume Method with Richards Equation

3.1 Modeling Moisture Content

We consider a sandy beach along a freshwater lake with a certain level of moisture content. Assume that the grain size of the sand is uniform throughout the beach. We also assume that there is a certain level of bacteria throughout this beach. These bacteria can be either mobile, that is, they move with the moisture between sand particles, or immobile such that they attach to sand particles and remain in place despite moisture movement through the sand [34]. Not only do some of the bacteria move with the moisture, but bacteria need moisture in order to survive and grow, so the bacteria population dynamics are dependent on the dynamics of the moisture in the beach. Richards Equation is a partial differential equation that models the movement of moisture through unsaturated soil. This equation has no known ana-

lytical solution, but the finite volume method can be used to approximate numerical solutions for this equation [6, 11, 17, 33].

To formulate Richards Equation, consider Darcy's Law describing the water flow rate through sand:

$$q = -K\nabla h,$$

where q, the vectorial quantity, is the flux or flow rate per unit area. This $q = \langle q_1, q_2 \rangle$ with q_1 as the x component of q and q_2 as the z component of q. While q is a vector quantity for three dimensions, for this model, we assume that everything behaves uniformly in the third dimension and therefore only consider the flux in the x and z directions. K is the hydraulic conductivity which measures the ease with which water can flow through the sand and is a function of water content and h is the pressure head [33]. When considering two dimensions, by mass conservation,

$$\frac{\partial \theta}{\partial t} + \nabla \cdot q = 0$$

$$\frac{\partial \theta}{\partial t} + \frac{\partial q_1}{\partial x} + \frac{\partial q_2}{\partial z} = 0$$

$$\frac{\partial \theta}{\partial t} = -\frac{\partial q_1}{\partial x} - \frac{\partial q_2}{\partial z}$$

where θ represents the volumetric water content, x is the horizontal direction and z is the vertical direction [6, 33]. Written another way,

$$\frac{\partial \theta}{\partial t} = \nabla \cdot \left(K\nabla(\psi + z) \right) \tag{3.1}$$

where ψ, the suction or matric potential, is a function of water content, and z is the gravitational potential for moisture due to capillary action. The gravitational

potential is measured as the height. The matric potential measures the ability of sand to suction moisture. [33].

We represent moisture on the volume element as dimensionless water content. Sand, especially below the surface of the beach, does not completely dry out, nor does it reach full saturation in natural conditions. Let θ_r be the residual water content, meaning the water content of the sand when it is as dry as natural conditions allow, and let θ_s be the saturated water content, or the highest water content that sand can achieve in natural conditions. These values are dependent on soil type and are obtained through experimentation and are readily available in the literature [1, 19, 27]. The dimensionless water content can be represented as [33, 35]:

$$\Theta = \frac{\theta - \theta_r}{\theta_s - \theta_r}, \qquad \theta_r < \theta < \theta_s.$$

Then (3.1) becomes,

$$\frac{\partial \Theta}{\partial t} = \frac{1}{\theta_s - \theta_r} \nabla \cdot \Big(K(\Theta) \nabla \big(\psi(\Theta) + z \big) \Big) \tag{3.2}$$

which gives an equation for the change in dimensionless water content [17, 35].

The models for matric potential and unsaturated hydraulic conductivity have been well-studied for over one hundred years and several different models have been proposed [26, 33]. In 1980, van Genuchten proposed the following model for the matric potential and it is a well-accepted model for this function [35]. This model is given as:

$$\psi(\Theta) = -\alpha \big(\Theta^{-1/m} - 1 \big)^{-1/n},$$

in terms of water content. α and n are all given as values estimated from data and $m = 1 - \frac{1}{n}$ [1, 3, 6, 19, 29, 33, 35, 36].

van Genuchten's model for the unsaturated hydraulic conductivity is also well-accepted and is given as [33, 35]:

$$K(\Theta) = K_0 \Theta^L \big(1 - (1 - \Theta^{1/m})^m\big)^2$$

where K_0 is the matching point saturation [33] and L is an exponent obtained through experimentation [3, 19, 29, 33, 35, 36, 42].

Integrating both sides of (3.2) over the domain D results in:

$$\int_D \frac{\partial \Theta}{\partial t} dD = \int_D \nabla \cdot \Big(\frac{1}{\theta_s - \theta_r} K \nabla (\psi + z)\Big) dD$$

$$\frac{\Theta_{i,j}^{t+\Delta t} - \Theta_{i,j}^t}{\Delta t} = \frac{1}{A} \int_S \vec{n} \cdot \Big(\frac{1}{\theta_s - \theta_r} K \nabla (\psi + z)\Big) dS \qquad (3.3)$$

where A is the area of the cell, S is the perimeter of the cell wall, and $\vec{n}$ is the outward normal vector to the cell wall.

3.2 Applying the Finite Volume Method to the Model

Since the bacterial content is dependent on moisture content, this model is driven by numerically solving (3.2). Figure 3.1 shows the domain mesh that is used and how this domain can be pictured in relation to a beach. It is assumed that the domain behaves uniformly in the third dimension just as this cross-section does.

Dirichlet boundary conditions that provide values for the moisture content of the boundary cells of the beach. The values of the matric potential, gravitational potential, and hydraulic conductivity on the walls of each of these cells are needed in order to obtain a solution. We can easily calculate the gravitational potential since it is just the height of each wall's center. The moisture values along the walls of each cell are needed since the matric potential and hydraulic conductivity are dependent on
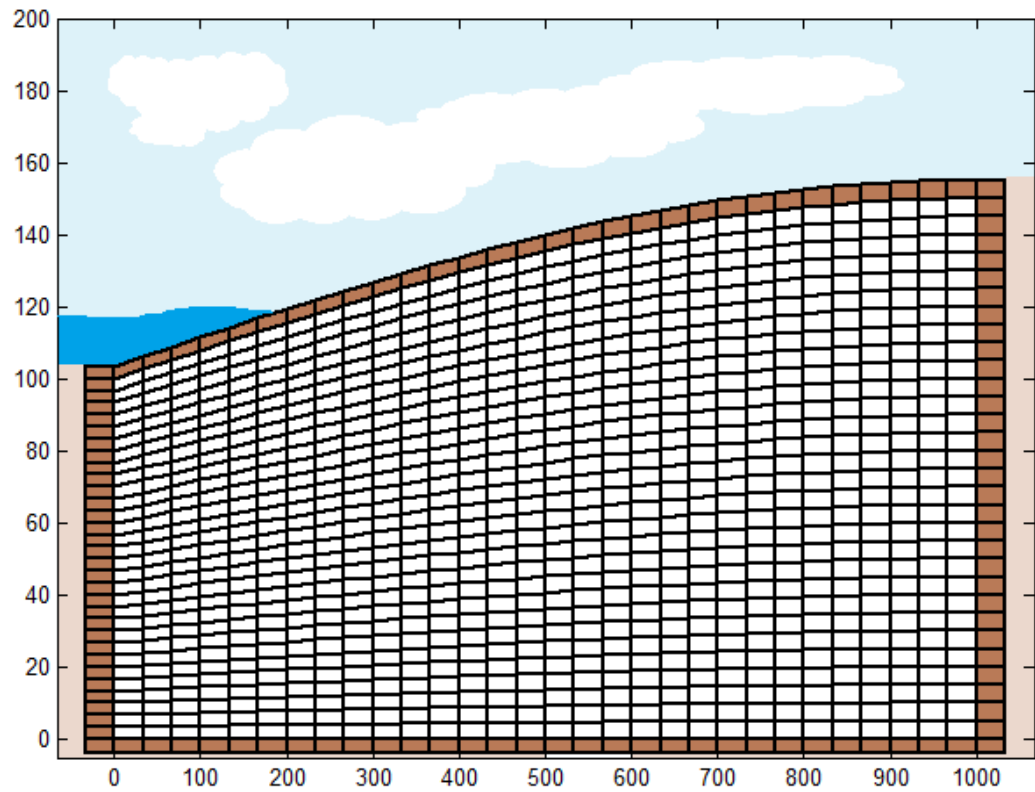
Figure 3.1: The above figure shows the domain used to represent a beach; divided into grid cells. The figure represents a cross section of the beach such that distance from the body of water is shown along the x-axis and depth of the beach is shown along the z-axis. These distances are measured in centimeters. The curve of the beach is represented by a sinusoidal curve. There is a depth of 100 cm on the left side of the domain and a depth of 150 cm on the right side of the domain. This represents the way a beach slopes leading to a body of water. The boundary cells are shaded and the domain itself is shown as white cells.

the moisture. The selected mesh is such that each quadrilateral cell has two vertical walls and the opposite walls of each volume element are either horizontal or slanted.
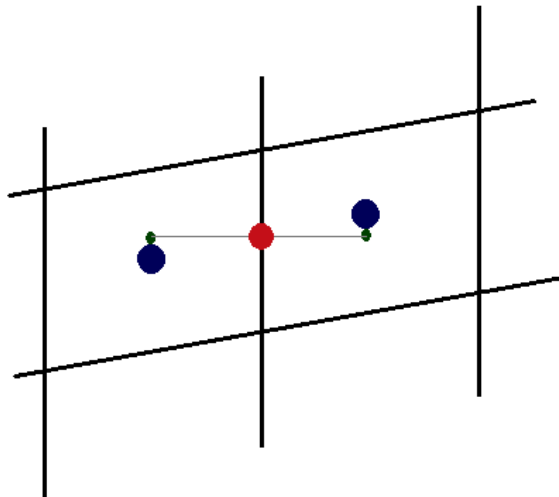
Figure 3.2: This figure illustrates how a moisture value is found along a vertical wall of one cell. In order to find the moisture value at the center point, Lagrangian interpolation is used to find the values (shown as smaller points) just above or below the respective cell centers. Then these values are averaged to find the needed moisture value along the vertical wall.

Consider the moisture values along the vertical walls as represented in Figure 3.2. We must find the moisture value on each vertical cell wall by using the moisture values for the center of each cell. Using Lagrangian interpolation, we can find the moisture values just above and below the centers. These moisture values are used to find the hydraulic conductivity, K, and the matric potential, ψ, in the x direction along all of the vertical walls. In order to find K in the z direction, the moisture used was that calculated along the horizontal or slanted walls by using an interpolation between the cell centers above and below the wall. The matric potential along these cell walls was averaged by the four matric potential values on the vertical walls around it as shown in Figure 3.3. It is important to note that small errors accumulated in this

interpolation can reduce the accuracy of the method.
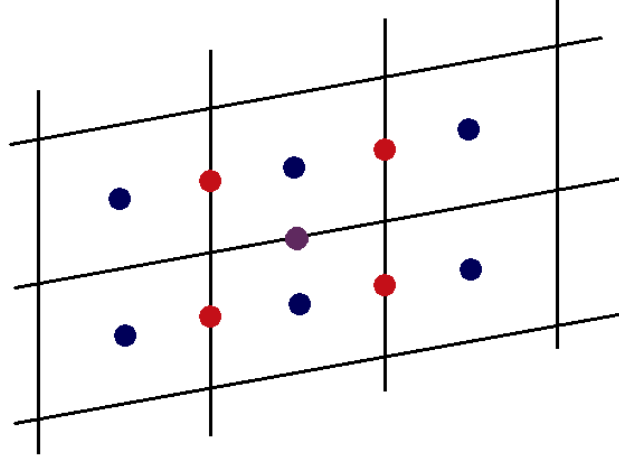
Figure 3.3: Here, the cell centers are shown as well as the locations along the vertical walls where the matric potential was calculated. These matric potential values are averaged to get the matric potential along the horizontal wall (this point shown in the very middle of the figure) to estimate the flux through the cell boundaries.

With the moisture values estimated on the center of the walls, the flux through the walls can be estimated. The outward unit normal along the vertical walls only has an x component. The projected component on to this normal is only the x component of this flux. For the horizontal or slanted walls, the normal component of the flux to that wall includes both x and z components. The outward unit normal vectors can be calculated based on the geometry of the selected mesh.

Equation (3.3) can be expanded as:

$$\frac{\Theta_{i,j}^{t+\Delta t} - \Theta_{i,j}^{t}}{\Delta t} = \frac{1}{A(\theta_s - \theta_r)} \int_S \vec{n} \cdot \langle K\psi_x, K\psi_z + K \rangle \, dS \tag{3.4}$$

Figure 3.4 identifies the positions around the walls of a cell. These positions are presented in a further discretization of equation (3.4) as follows:

Let W^a, W^b, W^c, and W^d be the widths of the walls going through the respective points a, b, c, and d. Let n_1 be the x component of the outward unit normal along each
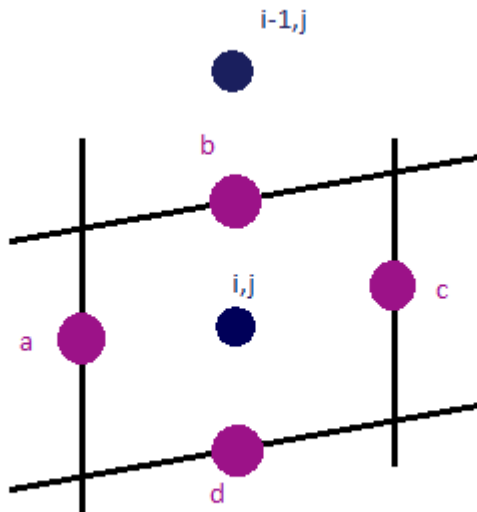
Figure 3.4: The above figure shows the positions on the cell walls contributing to the flux calculation as described in Equation (3.5).

wall and n_2 be the z component of the same normal. Note that $\langle n_1^a, n_2^a \rangle = \langle -1, 0 \rangle$ and $\langle n_1^c, n_2^c \rangle = \langle 1, 0 \rangle$. Then (3.4) becomes:

$$\Theta_{i,j}^{t+\Delta t} - \Theta_{i,j}^t = \frac{\Delta t}{A(\theta_s - \theta_r)} \int\limits_S \overrightarrow{n} \cdot \langle K\psi_x, K\psi_z + K \rangle \, dS$$

$$\Theta_{i,j}^{t+\Delta t} = \Theta_{i,j}^t + \frac{\Delta t}{A(\theta_s - \theta_r)} \int\limits_S \overrightarrow{n} \cdot \langle K\psi_x, K\psi_z + K \rangle \, dS$$

$$\Theta_{i,j}^{t+\Delta t} = \Theta_{i,j}^t + \frac{\Delta t}{A(\theta_s - \theta_r)} \Big(W^a K^a \big(\langle n_1^a, n_2^a \rangle \cdot \langle \psi_x^a, \psi_z^a + 1 \rangle \big)$$

$$+ W^c K^c \big(\langle n_1^c, n_2^c \rangle \cdot \langle \psi_x^c, \psi_z^c + 1 \rangle \big)$$

$$+ W^b K^b \big(\langle n_1^b, n_2^b \rangle \cdot \langle \psi_x^b, \psi_z^b + 1 \rangle \big)$$

$$+ W^d K^d \big(\langle n_1^d, n_2^d \rangle \cdot \langle \psi_x^d, \psi_z^d + 1 \rangle \big) \Big)$$

$$\Theta_{i,j}^{t+\Delta t} = \Theta_{i,j}^t + \frac{\Delta t}{A(\theta_s - \theta_r)} \Big(- W^a K^a \psi_x^a + W^c K^c \psi_x^c$$

$$+ W^b K^b \big(\psi_x^b n_1^b + \psi_z^b n_2^b + n_2^b \big) + W^d K^d \big(\psi_x^d n_1^d + \psi_z^d n_2^d + n_2^d \big) \Big)$$

Equation (3.5) represents the form of Richards Equation that was used to run the simulation.

$$\Theta_{i,j}^{t+\Delta t} = \Theta_{i,j}^t + \frac{\Delta t}{(\theta_s - \theta_r)A} \Big(\big(W^c K^c \psi_x^c - W^a K^a \psi_x^a \big)$$

$$+ \big(W^b K^b \psi_x^b n_1^b + W^b K^b \psi_z^b n_2^b + K_{i-1,j} n_2^b \big)$$

$$+ \big(W^d K^d \psi_x^d n_1^d + W^d K^d \psi_z^d n_2^d + K_{i,j} n_2^d \big) \Big) \qquad (3.5)$$

The values of $K_{i,j}$ and $K_{i-1,j}$ are used instead of the K values directly on the walls as an upwinding scheme. By using the height of the center of the cell above the wall for this value, the moisture is encouraged to move down through the domain during the simulation.

4 Modeling Bacterial Growth

For this model, it is assumed that bacteria only need water and nutrients to survive. Here we focus on the specific bacteria *Escherichia coli*, commonly, *E. coli*, which are

either mobile or immobile in the media. Currently, the interactions between most bacteria, moisture, and nutrients is not fully understood. While it is known that bacteria prefer to grow in certain conditions, the effect of these varying conditions on bacterial growth is a complicated area of study [6, 15, 18, 20, 24, 37, 39, 40]. For simplicity, we assume that the temperature is within the correct range necessary for bacterial growth and survival.

It is possible for bacteria that are mobile in the water to become immobile by attaching to grains of sand. While immobile, bacteria can grow, shedding mobile daughter cells into the water. Although attachment of bacteria is somewhat studied, detachment is a topic that is explored less often [34]. We will consider two subpopulations of the total bacteria population. Bacteria are either mobile and can move between grains of sand when fluxed with the moisture, or they are immobile. Immobile bacteria do not move with the moisture flux, but still need favorable moisture conditions to survive and grow. Assume that there are rates at which bacteria attach and detach from the sand. The following system is used to model the bacteria and nutrient contents in the beach:

$$\frac{\partial B_m}{\partial t} = \nabla \cdot \big(\xi_1 B_m K \nabla(\psi + z)\big) + (\mu - d_1 - \gamma_1)B_m + (\mu + \gamma_2)B_i,$$

$$\frac{\partial B_i}{\partial t} = \gamma_1 B_m - (d_2 + \gamma_2)B_i,$$

and,

$$\frac{\partial N}{\partial t} = \nabla \cdot \big(\xi_2 N K \nabla(\psi + z)\big) - \varepsilon \mu B,$$

where B_m is the concentration of mobile bacteria, B_i is the concentration of immobile bacteria, and the total concentration of bacteria is given as $B = B_m + B_i$. The concentration of nutrients is represented as N. The units for, or expression of, measuring

the concentration of bacteria in sand is not universally agreed upon [38]. For the purposes of this paper, we express the concentration of bacteria in colony forming units (CFU's) per 100 cm^3 of sand. We also assume the nutrient levels are measured in μmol per 100 cm^3 of sand. We use ε as a proportionality constant that scales the bacteria's uptake of nutrients. This ε can be adjusted depending on the situation and the actual value for this parameter is a subject of further study. The parameters ξ_1 and ξ_2 denote the transport rates for the mobile bacteria and the nutrient, respectively, and represent the impact the moisture flux has on moving mobile bacteria and nutrients through the sand. The rate that mobile bacteria become immobile is represented as γ_1 and the rate at which immobile bacteria become mobile is represented as γ_2. The rate at which mobile bacteria die is given as d_1 and the rate at which immobile bacteria die is given as d_2.

μ is a function of water content and nutrient levels and represents the growth rate of the bacteria population [6, 24]. It is more specifically represented as:

$$\mu = \mu_{max} f(\Theta) \frac{N}{C_N + N},$$

where C_N is a nutrient parameter, μ_{max} is the greatest rate at which bacterial growth can occur, and there is a range of moisture that promotes bacterial growth modeled by some function $f(\Theta)$ [6, 24]. Little is known regarding the bacterial growth dependence on moisture except for general relationships and the fact that bacteria need water to thrive and grow. We will thus consider four functions as follows and compare the results of simulations using these functions for $f(\Theta)$:

$$f_1(\Theta) = 0.765 \left(\frac{1}{2\pi\sigma^2} e^{-\frac{1}{2\sigma^2}(\Theta - \Theta_{opt})^2} \right)$$

$$f_2(\Theta) = 1 - e^{-5\Theta}$$

$$f_3(\Theta) = 0.425 \left(\frac{\Theta^{a_1-1}(1 - \Theta^{b_1-1})}{B(a_1, b_1)} \right)$$

$$f_4(\Theta) = 0.513 \left(\frac{\Theta^{a_2-1}(1 - \Theta^{b_2-1})}{B(a_2, b_2)} \right)$$

The scalars in the beginning of $f_1(\Theta)$, $f_3(\Theta)$, and $f_4(\Theta)$ were approximated so that at the optimal moisture level the $f(\Theta)$ will result in a value of one; making a comparison of these functions possible. The $f_1(\Theta)$ is a scalar density function of the normal distribution centered around Θ_{opt}. This function results from the assumption that the bacteria need a higher level of moisture, but levels that are too high will result in less bacterial growth. The $f_2(\Theta)$ was chosen to see if there was a pattern of more moisture relating to more bacterial growth with bacteria preferring the highest moisture level possible. The functions $f_3(\Theta)$ and $f_4(\Theta)$ are both based on the Beta Distribution. $f_3(\Theta)$ was chosen to see if there is a very strong preference for a high relative moisture level, but with growth quickly decreasing beyond that level. Although intuitively it would seem that a higher moisture level would be preferable for the bacterial growth, $f_4(\Theta)$ was chosen to investigate any preference the bacteria might have for growing where there is moisture, but not so much that it is overwhelming to their growth. The goal is to see if the pattern of bacterial growth found when using any or all of these functions follows the results that are shown in the literature. A visualization of these four curves in relation to the moisture level is given in Figure 4.1.
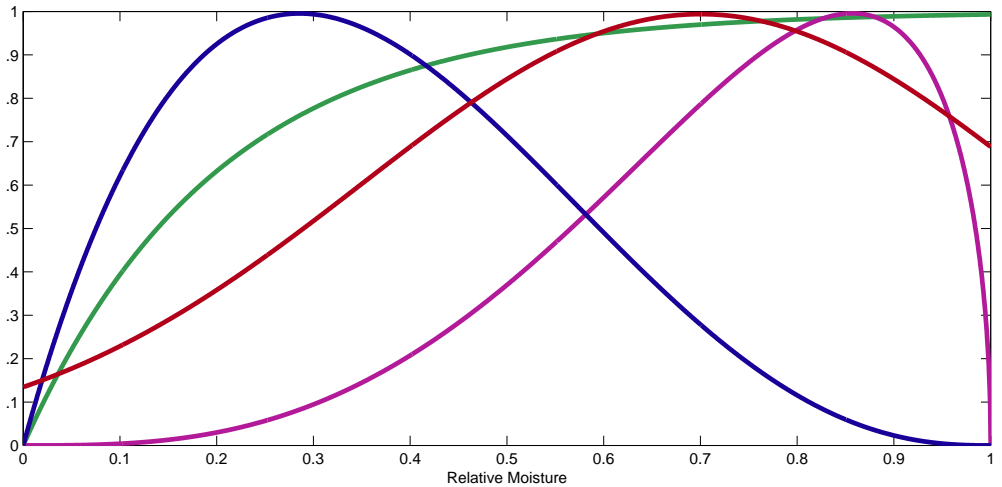
Figure 4.1: The above shows the bacterial growth factor as a function of the relative moisture content. $f_1(\Theta)$ is represented in red, $f_2(\Theta)$ is represented by the green curve, $f_3(\Theta)$ is represented by the purple curve, and $f_4(\Theta)$ is represented in blue. The parameters used are $\Theta_{opt} = 0.7$, $a_1 = 4$, $b_1 = 1.5$, $a_2 = 2$, and $b_2 = 3.5$.

5   Results

5.1   Simulation of Moisture

The simulation of bacteria and nutrient dynamics is driven by the moisture dynamics[1].

Thus, the first consideration was to properly simulate how moisture flows through the

beach. Since Richards Equation models moisture movement in unsaturated soils, if

the cells in the discretized beach become too saturated, the simulation does not give

biologically relevant results. This means that, for our simulation, while the boundary

cells can be nearly completely saturated, moisture can still flow through the sides and

out of the bottom of the domain. The initial moisture profile is given by an equation

using the arctangent function and is shown in Figure 5.1.

The model was tested using some fully saturated moisture values in an attempt

---

[1]A PDF of the MATLAB code used to run these simulations is available upon request by emailing the author at tewinke2@uwm.edu.
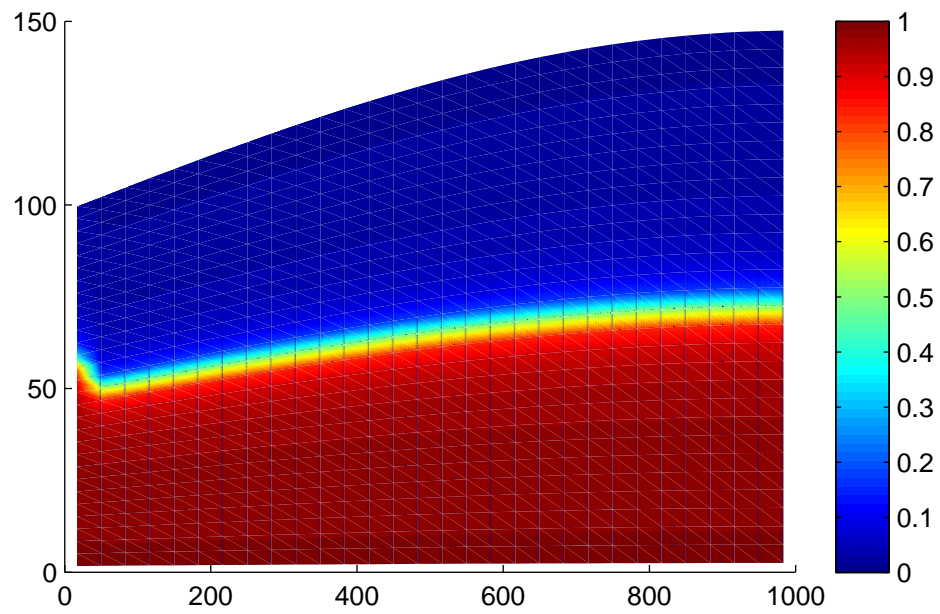
Figure 5.1: The above shows the initial moisture profile at the beginning of each simulation given as relative moisture content. There is no wave wetting at the start of the simulation and it is assumed that ground water would flow below the x-axis in this domain.

to flood the beach and impossible moisture values resulted due to the fact that the moisture model is only for unsaturated soil. So, we focused on keeping the simulations such that all values for moisture, nutrient, and bacteria are within biological possibility. Simulations were done both with and without rain wetting and all simulations were run with a wave wetting. For the simulation of wave wetting, the top boundary conditions for the first cells (approximately the first 333 cm of the domain) on the left side were given a relative moisture value of 0.95 for a certain period of time every minute depending on how close to the body of water the respective domain cell was. To simulate a rain type of wetting, the entire top boundary was changed to have a relative moisture content of 0.95 for the duration of the simulation of this type of wetting. When boundary wetting does not occur, the appropriate top boundary cells are turned to the default top boundary value of 0.1. It should be noted that this is not a completely accurate way to model waves and rain. This is why we refer to it as either wetting or dampening. In reality, when water is added to the top of a beach, a saturated column develops in the top layers and the pressure increases, thus encouraging the water to push through the sand. The situation gets more complicated when we consider that sometimes it rains very heavily and other times there is just light rain. Our simulation does not account for differences between wetting events. It simulates rain and waves by just adding moisture to the system as a Dirichlet boundary condition.

Since the nutrients and bacteria have a flux dependence, when the rain dampening is simulated, extra nutrients and bacteria are added to the system at the boundaries along with the moisture. When it rains in reality, runoff comes down the beach and brings in extra nutrients and bacteria, so this is appropriate for the model. The values for modeling moisture have been established and are shown in Table 5.1 [1, 3, 6, 19, 29, 33, 35, 36, 42].

It is assumed that no bioclogging occurs. In other words, the population of bacte-

Table 5.1: Constants for Modeling Moisture Movement

K_0	L	α	n	θ_r	θ_s
29.7	-0.930	0.145	2.68	0.045	0.43

ria cannot become so great that the cells block moisture movement through the beach. No matter how we simulate bacterial growth, moisture movement is not affected. Although bioclogging does occur in certain situations [5, 28, 34], the complexity that it adds to the model was beyond the scope of this paper.

The boundary conditions related to the relative moisture content are as follows: the top boundary has a moisture level of 0.1, the bottom boundary has a moisture level of 0.98, the left boundary has a moisture level of 0.99, and the right moisture level if 0.75. Figure 5.2 shows the moisture profile after twenty-four hours of only wave dampening. The effect of this dampening on the left can be seen as well as the moisture moving through the bottom of the domain when compared to Figure 5.1.

Next, a twenty-four hour period was simulated with rain dampening from hour one to hour nineteen only. Throughout the simulation the moisture seeps into the domain as provided by the rain and wave wetting boundary conditions. The wave movement continues throughout the entire simulation. Moisture moves down and to the right of the beach profile as would be expected. The beach profile after a total of fourteen hours is shown in Figure 5.3. Figure 5.4 shows the domain profile after twenty-four hours.

The moisture flux through the top boundary was tracked through both simulations and was consistently positive for all moisture simulations. The rain moisture continues to move moisture deeper into the sand as it is pulled down by gravity. In a more complicated model, rain and waves would be modeled by an increase in water on the top boundary as well as an increase in pressure which would cause moisture to be pulled down through the domain even more than what is shown here. Adding this
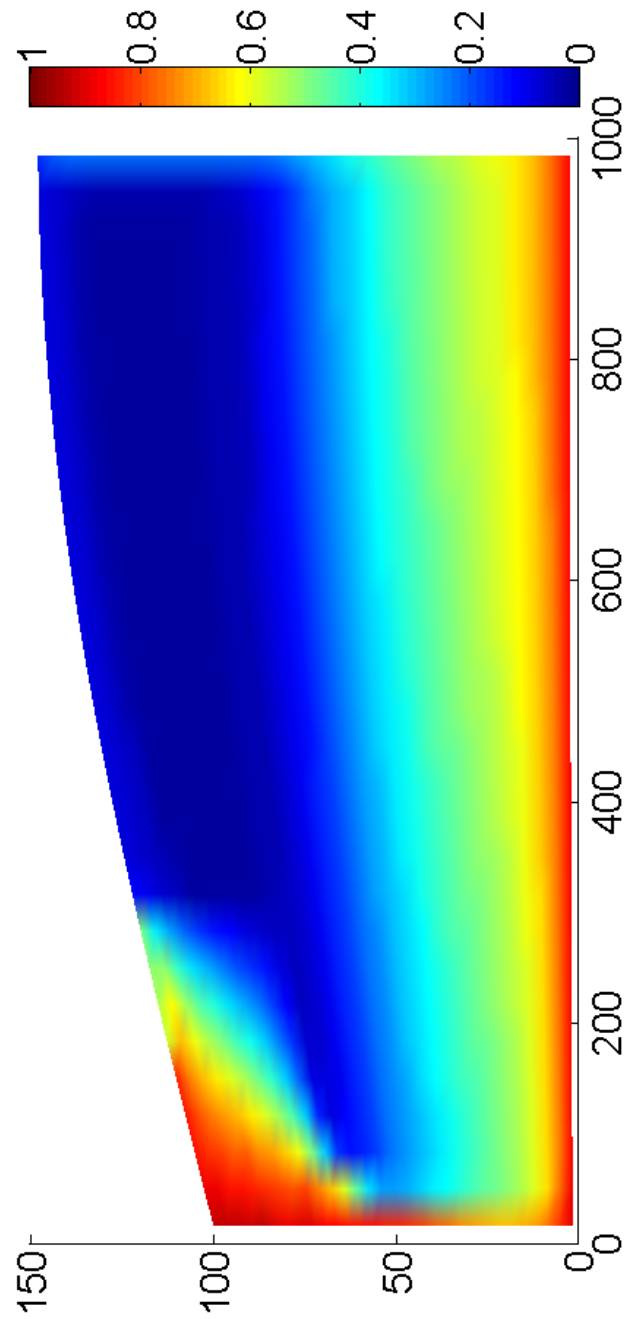
Figure 5.2: This figure shows the moisture profile as a result of simulating a twenty-four hour period with only wave wetting. This addition of moisture via wave dampening continued for the entire simulation.
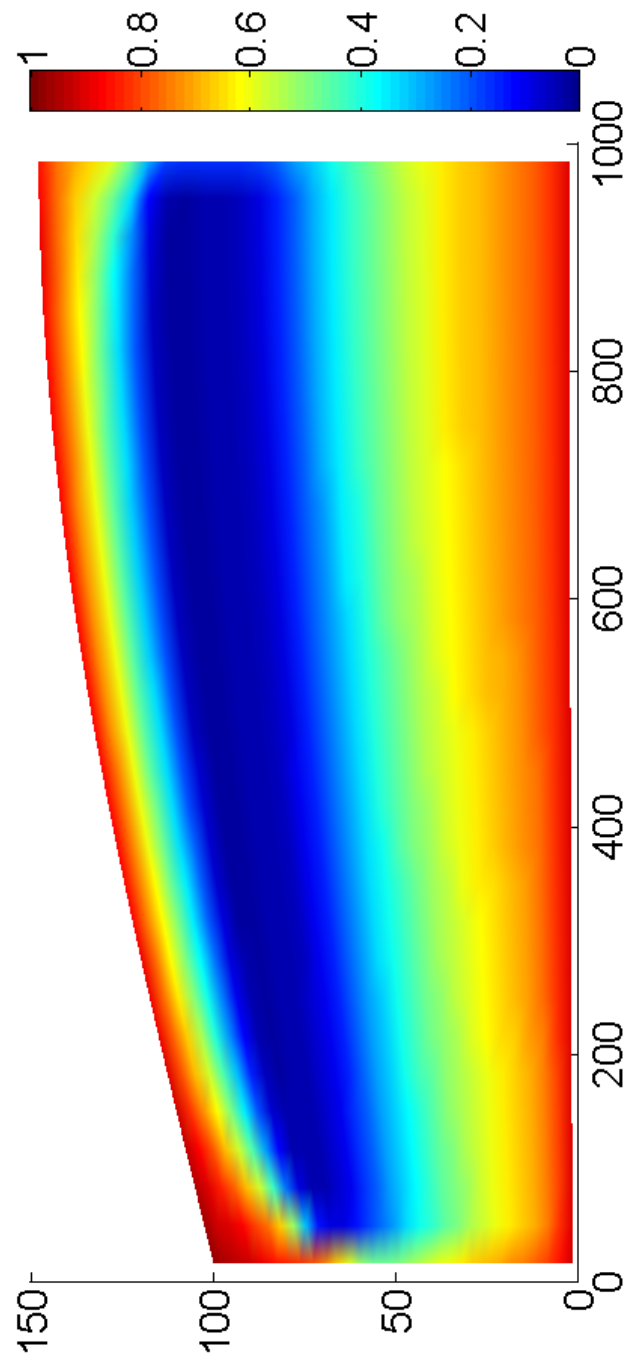
Figure 5.3: This profile was produced after a thirteen hours of simulated rain wetting. The top of the profile is near saturation and the moisture seeps down the domain.
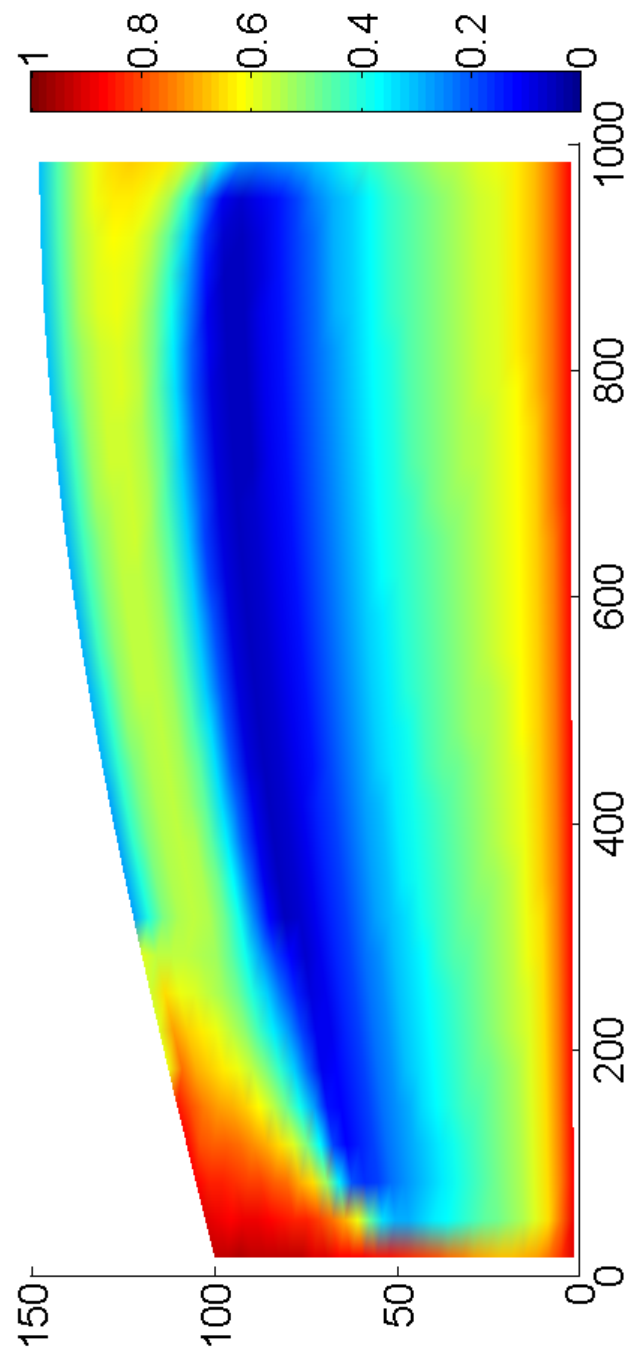
Figure 5.4: This figure shows the moisture profile after twenty-four simulated hours. A rain dampening was simulated from hours one to nineteen. Moisture is seen seeping into the sand, but the top of the domain is dry due to changed boundary conditions.

component would be appropriate in a continuation of this research.

5.2   Simulation of Bacterial Growth

5.2.1   Initial and Boundary Conditions

Since nutrient can move with the flux, it is assumed for the initial conditions that it has done just that. Also, it was assumed that there is some uniform level of nutrient for all cells at the start of the simulation. The initial conditions for the nutrient are shown in Figure 5.5. The nutrient boundary conditions are kept simple as zero on all borders except for a nutrient content of one for the top boundary. The same boundary conditions hold for the bacteria. These conditions ensure that bacteria and nutrient are not added through the boundary conditions on the bottom or sides of the domain. Exploring the effect of varying the boundary conditions is a topic for further work.

Since mobile bacteria need moisture to move, it was assumed there is a greater moisture dependence for the mobile bacteria than for the immobile bacteria. There are thus more mobile bacteria in the cells with a higher moisture level. We also assumed that there is some uniform distribution of mobile bacteria to all cells since there is some level of moisture in all cells. The initial mobile bacteria distribution is shown in Figure 5.6.

Although immobile bacteria need moisture to survive, it is within reason to assume that some mobile bacteria traveled through the moisture to a particular cell in the domain, attached to the sand in that cell, and remained there even after some of the moisture traveled away from the cell. Therefore, we assumed that there is a greater number of immobile bacteria uniformly distributed and there are fewer bacteria distributed based on relative moisture level. Figure 5.7 shows the initial immobile bacteria distribution and the total initial bacteria distribution is shown in Figure 5.8.
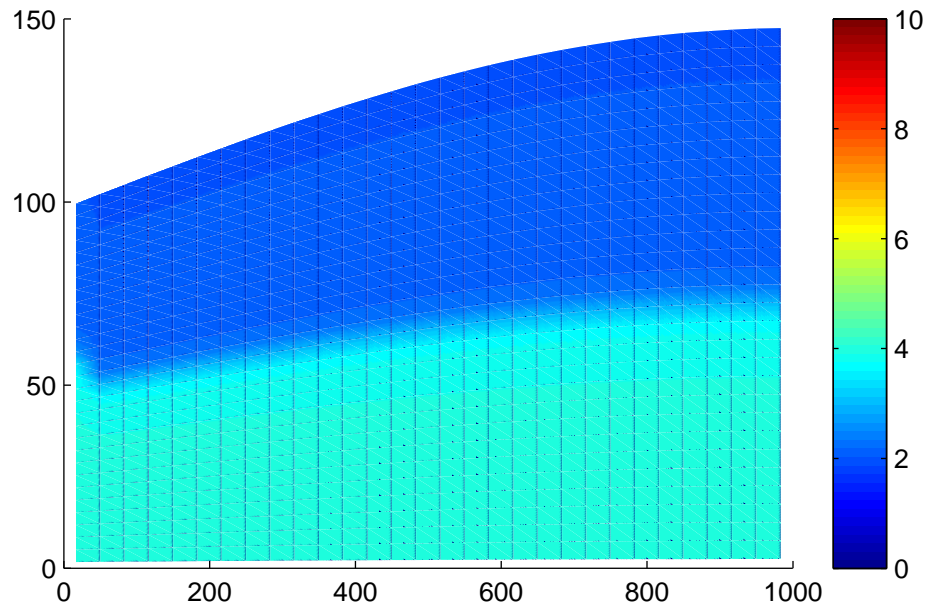
Figure 5.5: The initial nutrient profile is shown above. The nutrient is measured in concentration of μmol per 100 cm^3 of sand.
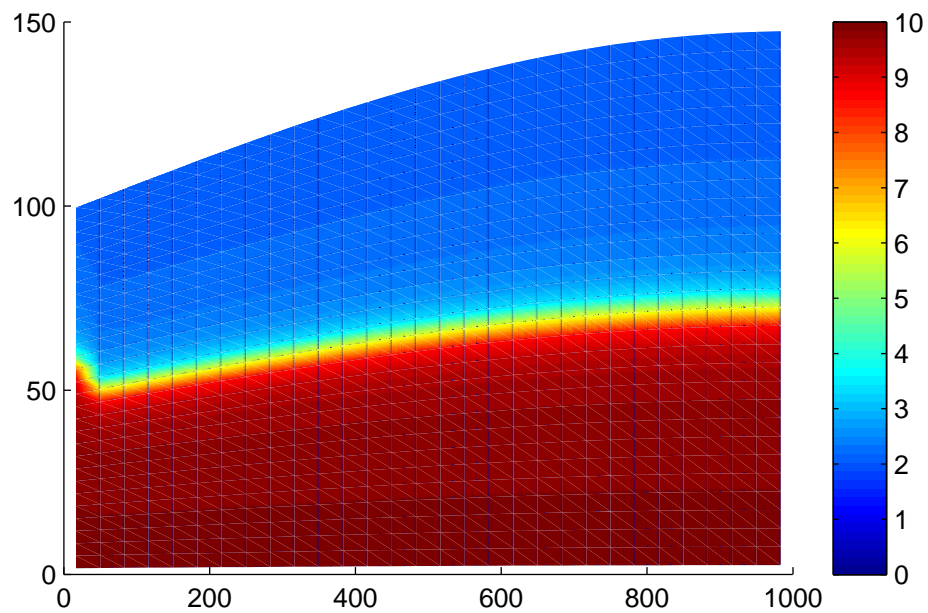

Figure 5.6: The above shows the initial mobile bacteria distribution. The bacteria is measured in concentration of CFU's per 100 cm^3 of sand.
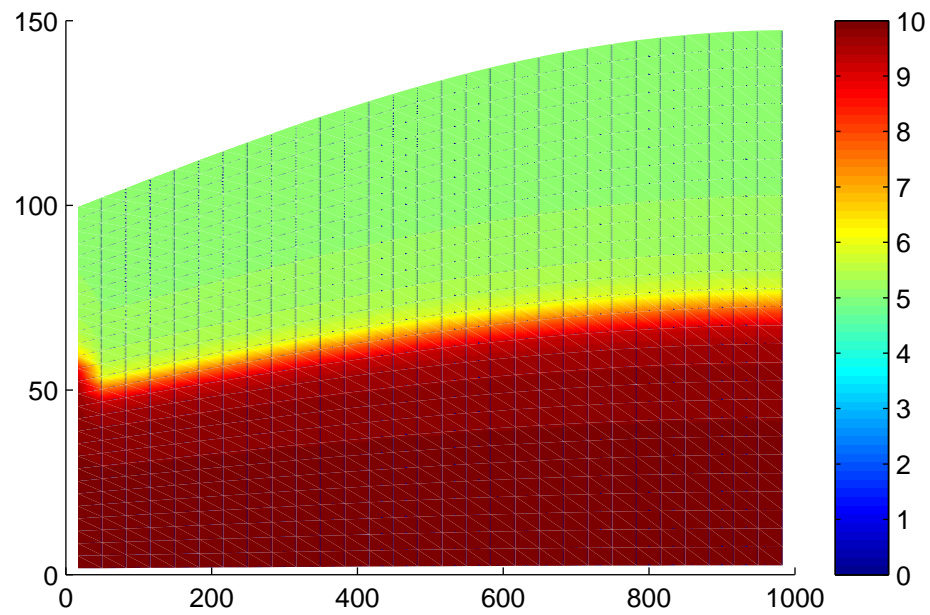
Figure 5.7: The above shows the immobile bacteria distribution at the start of each simulation.
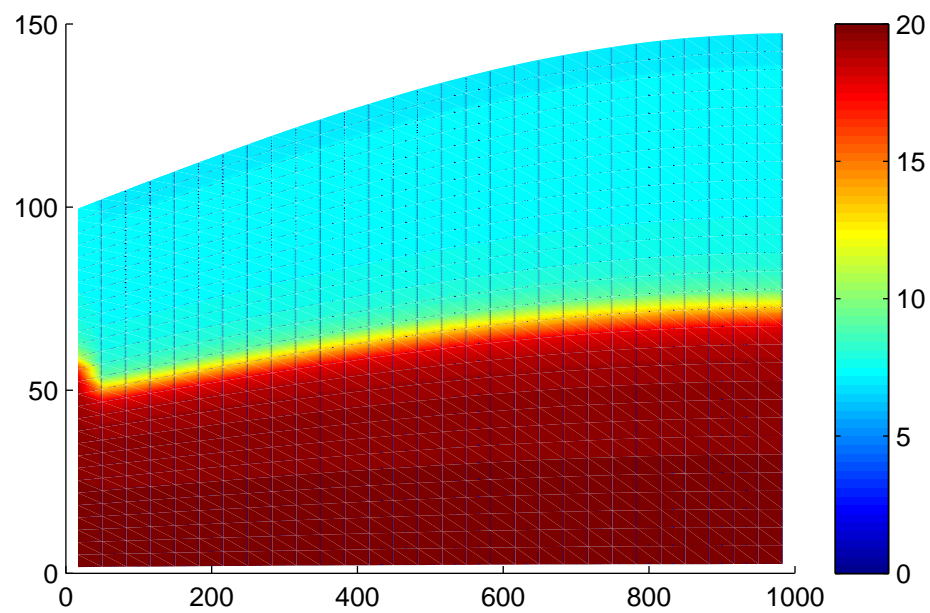

Figure 5.8: The above shows the total bacteria distribution at the start of each simulation.

Table 5.2 shows the parameter values used in conjunction with the nutrient and bacteria modeling.

Table 5.2: Constants for Modeling Bacterial Growth and Nutrients

C_N	μ_{max}	ξ_1	ξ_2	σ	d_1	d_2	γ_1	γ_2	ε	Θ_{opt}
30	30	0.2	0.1	0.35	3	2	3	1	0.3	0.7

5.2.2   Results With No Rain

The first simulations were run with only wave dampening. Figure 5.9 shows the results after a twenty-four hour simulated period using $f_1(\Theta)$ as the moisture-dependent growth factor. Most of the bacterial growth is toward the bottom half of the domain and where the wave dampening has added moisture.

Figure 5.10 shows the results of running the same simulation with $f_2(\Theta)$ as the moisture-dependent bacterial growth factor. There is slightly more growth in the bottom half of the domain than with the simulations using $f_1(\Theta)$, but the growth is approximately the same. Figure 5.11 shows the results of the same simulation for the nutrients. There is not much change from the initial nutrient profile at about fifty centimeters of depth, but below that, some of the nutrient has been consumed by the bacteria in that part of the domain. There is also a little nutrient that was fluxed in with the wave wetting. The nutrient profile is not shown for the other simulations, but they all follow the pattern of less nutrient remaining where more bacteria has grown and some nutrient added where wave dampening has occurred. During the simulation, some bacteria and nutrient can be seen exiting through the bottom of the domain as they travel with the moisture flux.

Figure 5.12 shows the results the bacterial growth for the simulation using $f_3(\Theta)$. The results show lower bacteria counts, although they are in the same areas of growth for the previous simulations. This difference is not wholly unexpected since much of

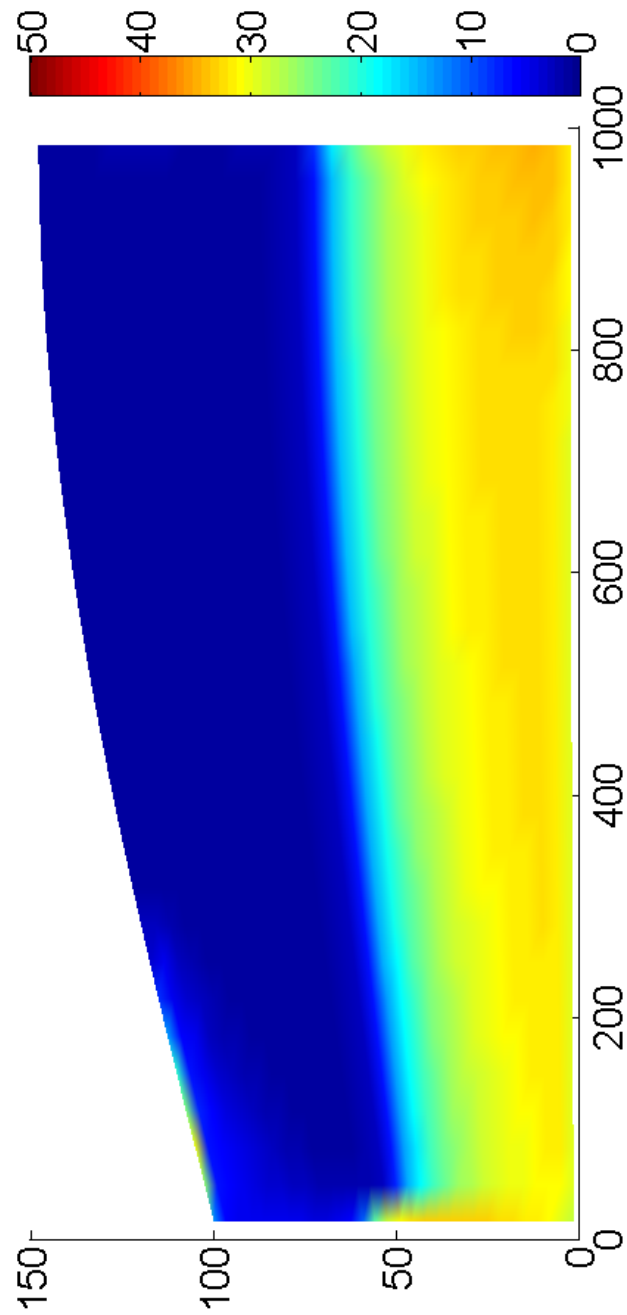Figure 5.9: This figure shows the bacteria profile after twenty-four hours of simulation with no rain dampening and using $f_1(\Theta)$.
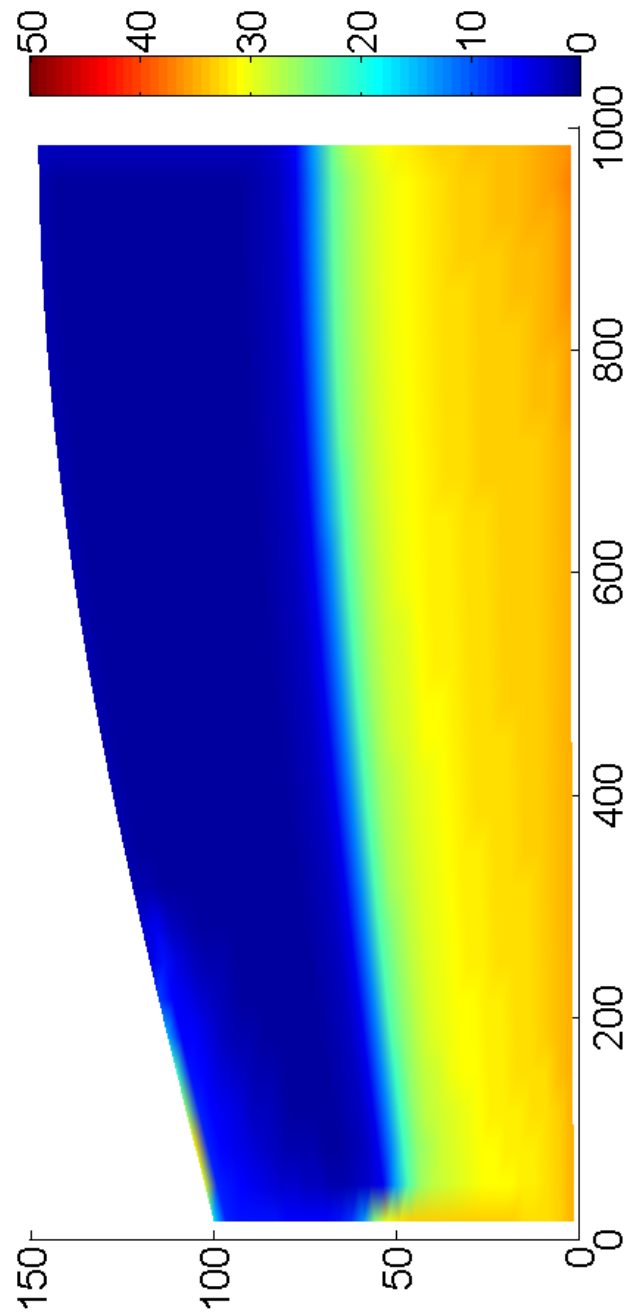
Figure 5.10: The above figure shows the bacteria profile after a simulated twenty-four hour period with no rain wetting and using $f_2(\Theta)$.
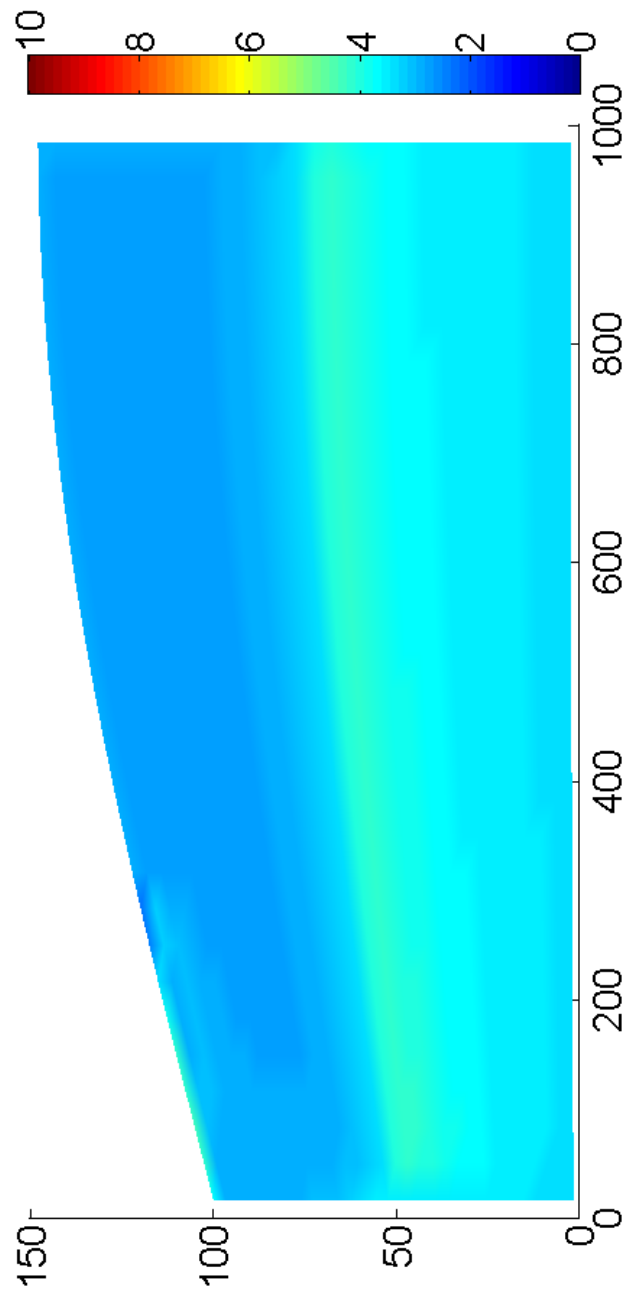
Figure 5.11: The above figure shows the nutrient profile after a simulated twenty-four hour period with no rain wetting and using $f_2(\Theta)$.

the moisture has moved through the domain and $f_3(\Theta)$ has much more of a clear preference for high moisture values than the other moisture-dependent bacterial growth functions.

The result of the bacteria growth simulation using $f_4(\Theta)$ is shown in Figure 5.13. There is much less growth for this moisture-dependent growth function and the scale was changed compared to the other simulations in order to more easily see where growth was occurring. The bacteria do not prefer to grow where moisture is added and the most obvious area of growth is seen as a band at about fifty centimeters depth. The concentration of bacteria in that part of the domain is about the same as the concentrations in that area for the simulations using $f_1(\Theta)$ and $f_2(\Theta)$. However, Figure 5.13 also shows that bacteria modeled by $f_4(\Theta)$ do not prefer to grow much below seventy centimeters depth unlike all three of the other simulations. Simulations of bacterial growth with $f_4(\Theta)$ shows a clear preference to grow at relative moisture values below 0.5, so it makes sense that there is less growth in areas of higher moisture. This low moisture preference prevents bacterial growth.

Since moisture, bacteria, and nutrient can move through the boundaries of the domain, the amount of nutrient and bacteria that passed through the domain boundary was tracked throughout the simulation. The flux of the bacteria through the domain boundaries when using $f_2(\Theta)$ is shown in Figure 5.14 and the flux of the nutrient through the domain boundaries when using the same moisture-dependent bacterial growth function is shown in Figure 5.15.

In order to get Figures 5.14 and 5.15, the flux through the bottom, right, and left boundaries is plotted time step for time step. For the the nutrient and bacteria flux through the top boundary, these fluxes were averaged every hour and plotted. When the top boundary bacteria and nutrient fluxes are plotted time step for time step, there are oscillations in the amount of bacteria and nutrient moving through the boundary in conjunction with the wave movement, but it was somewhat difficult to see
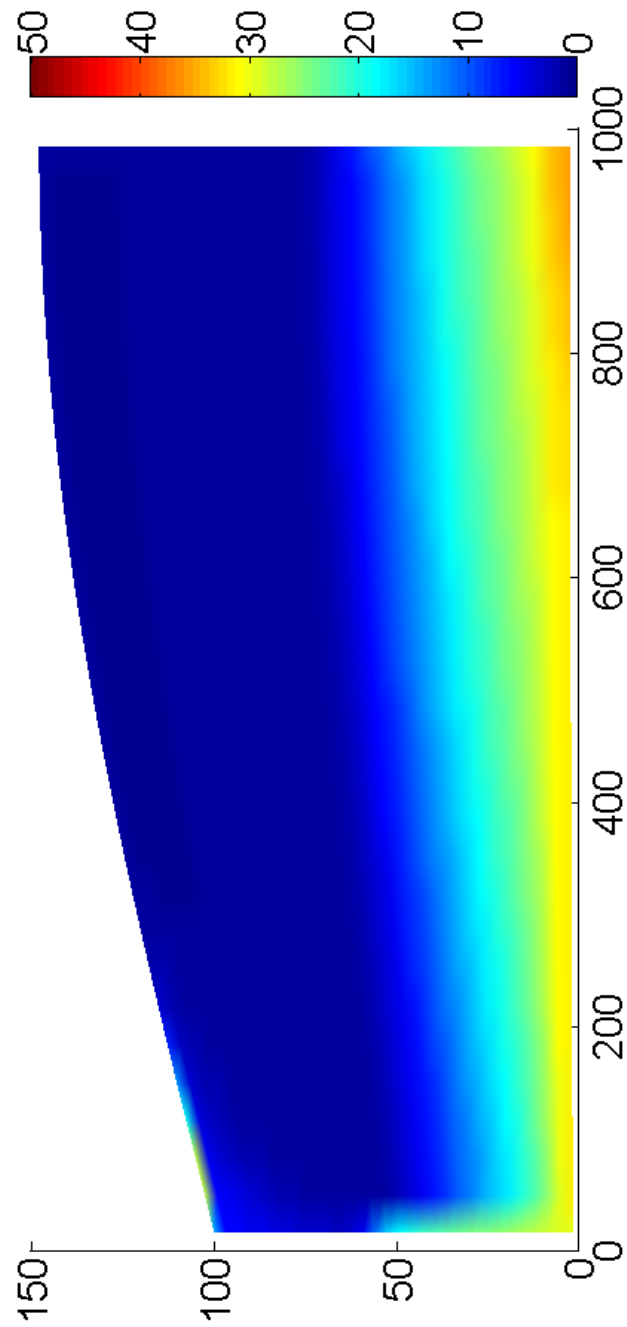
Figure 5.12: This figure shows the bacteria profile as a result of simulating a twenty-four hour period using $f_3(\Theta)$. There was only a wave wetting used in this simulation.
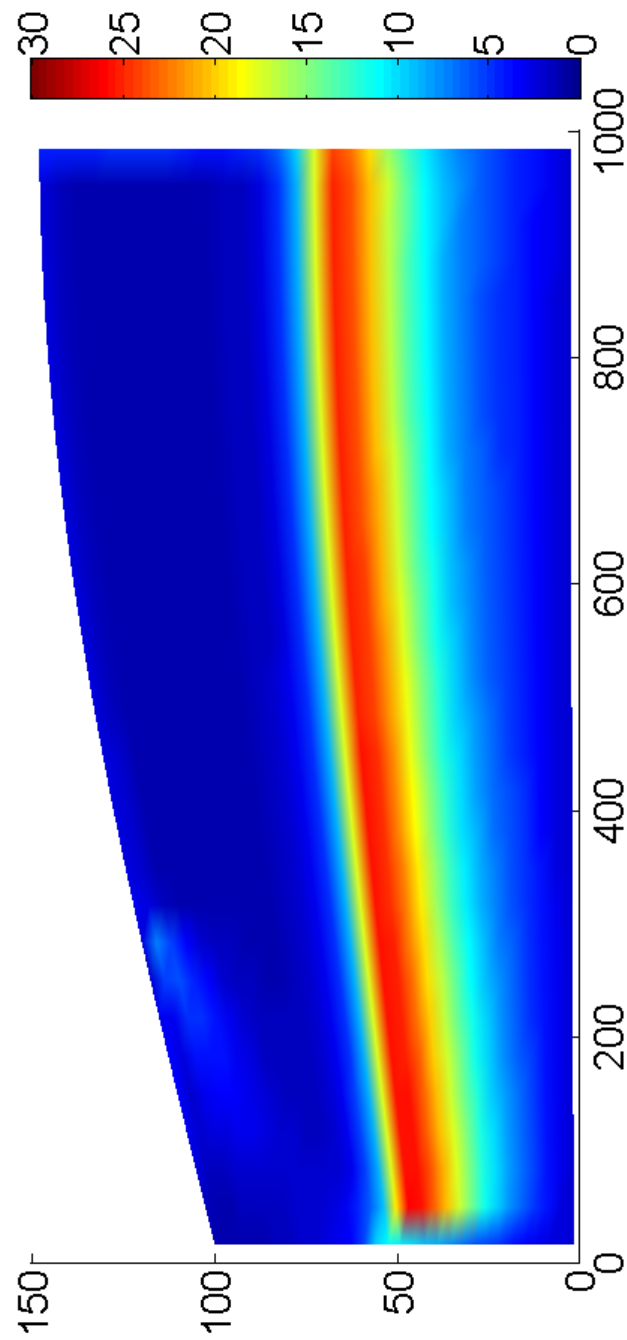
Figure 5.13: The above shows the bacteria profile as a result of simulating a twenty-four hour period using $f_4(\Theta)$ with only wave wetting.

that, overall, bacteria and nutrient were added through the top domain. Therefore, we took an average of the amount of bacteria and nutrient being fluxed through the top boundary.

Figure 5.14: The above shows the bacteria fluxed through the domain boundaries as a result of simulating a twenty-four hour period using $f_2(\Theta)$ with only wave wetting.

The wave dampening is simulated by only having Dirichlet boundary conditions, so when cells are not experiencing a wave dampening, the top boundary has a moisture value of 0.1. This causes some of the moisture that was added during the dampening to be suctioned back through the top of the domain by matric potential and this suctions back some of the nutrient and bacteria out of the domain; resulting oscillations when the flux values are plotted. Dirichlet boundary conditions used in this manner are not the most effective way of modeling wave movement since the suctioning of flux back through the top of the domain does not happen with actual lake waves. However, on average, it can still be seen in these figures that nutrient and bacteria are being added in small amounts through the top boundary during the simulation
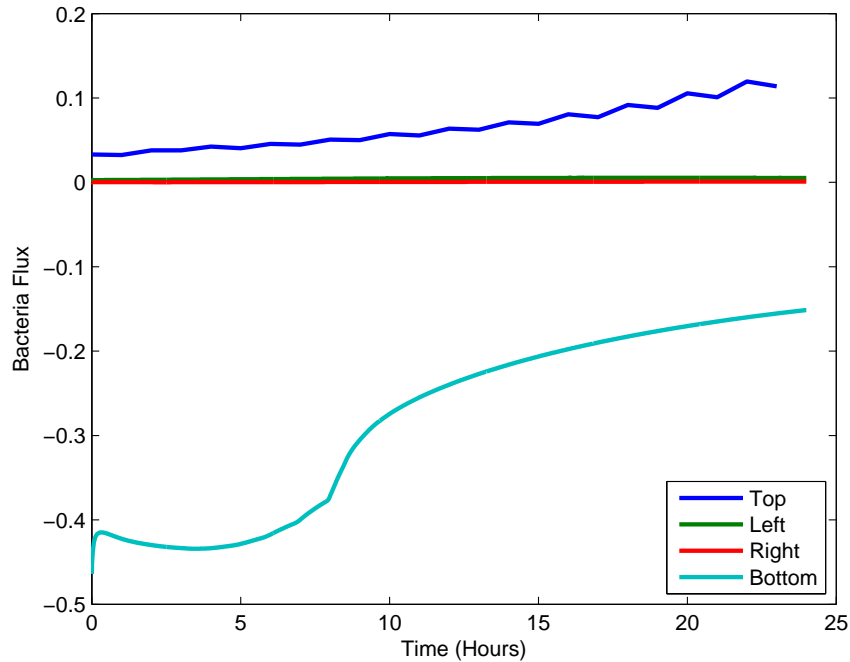
due to the wave dampening.
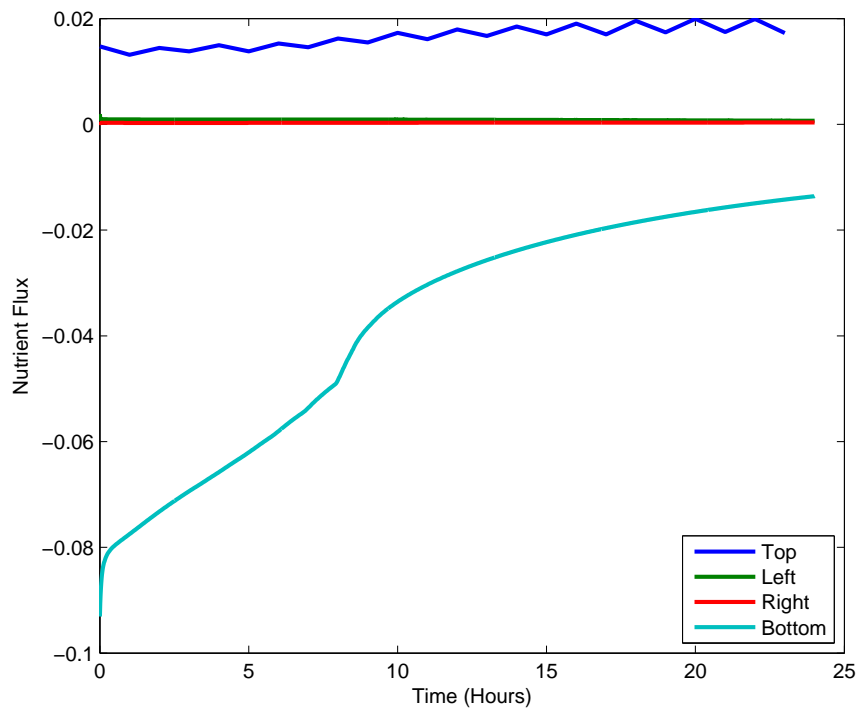
Figure 5.15: The above shows the nutrient fluxed through the domain boundaries as a result of simulating a twenty-four hour period using $f_2(\Theta)$ with only wave wetting.

For all of the simulations in this section, the most bacteria and nutrient is lost through the bottom boundary of the domain. At no point did the domain lose or gain more than one CFU of bacteria per 100 cm^3 or one μmol per 100 cm^3 of nutrient through any boundary. Most of the loss was from the moisture fluxing through the bottom boundary and was experienced within the first simulated ten hours. This corresponds to when most of the moisture is lost through the bottom of the domain. Bacteria and nutrient were lost through the right and left sides of the domain in trivial quantities. The addition of bacteria to the system through the top is not enough to account for the growth seen in the simulations where there is wave dampening.

5.2.3   Results With Rain

Next, the simulation was run for the same period of time, but with eighteen hours of rain wetting simulated from hours one to nineteen. Figure 5.16 shows the results of using $f_1(\Theta)$ to model moisture-dependent bacterial growth. Note that the scale was changed from the previous section in order to properly see approximately what the bacteria counts are in the highest region of bacterial growth. It is clear that there is much more growth as a result of the increase in moisture. Almost all of the growth is shown to be where the moisture levels were increased as a result of the changed boundary conditions in the simulation. Growth below the surface matches that in the previous section, so it is only growth on the surface of the beach that is affected. This makes sense because rain dampening causes moisture to seep into the beach and make a better living environment for the bacteria. Studies show that there is a great spike in bacterial growth following a rain event, sometimes resulting in very dangerous bacteria levels [5, 6, 34, 38]. This is partly due to bacteria and nutrient added to the system, but is also due to the increase in favorable growing conditions by the increase in moisture in the sand.

The results when running the same simulation with $f_2(\Theta)$ are shown in Figure 5.17. The amount of growth and location of growth is very similar to that shown in Figure 5.16. Figure 5.18 shows the corresponding nutrient profile for the beach. The nutrient profiles for the other simulations are not shown, but at the end of each simulation, where there was increased bacterial growth, there is less nutrient remaining and there is some nutrient added with the flux on the top boundary.

The results for the same simulation using $f_3(\Theta)$ are shown in Figure 5.19. It is almost indistinguishable from Figure 5.16. As with the previous simulations involving rain, the bacteria's high moisture preference and the influx of moisture result in excellent conditions for growth. The area where there is wave dampening shows the
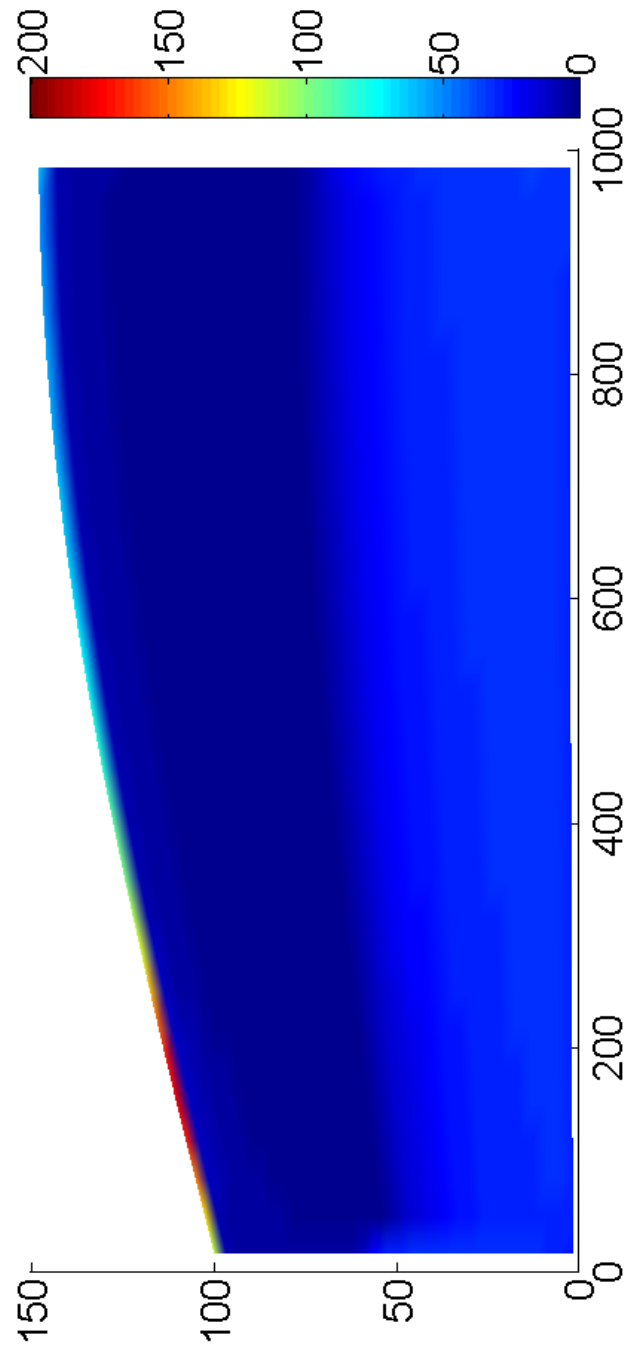
Figure 5.16: This figure shows the result of simulating a twenty-four hour period using $f_1(\Theta)$. From hours one to nineteen, rain wetting was simulated.
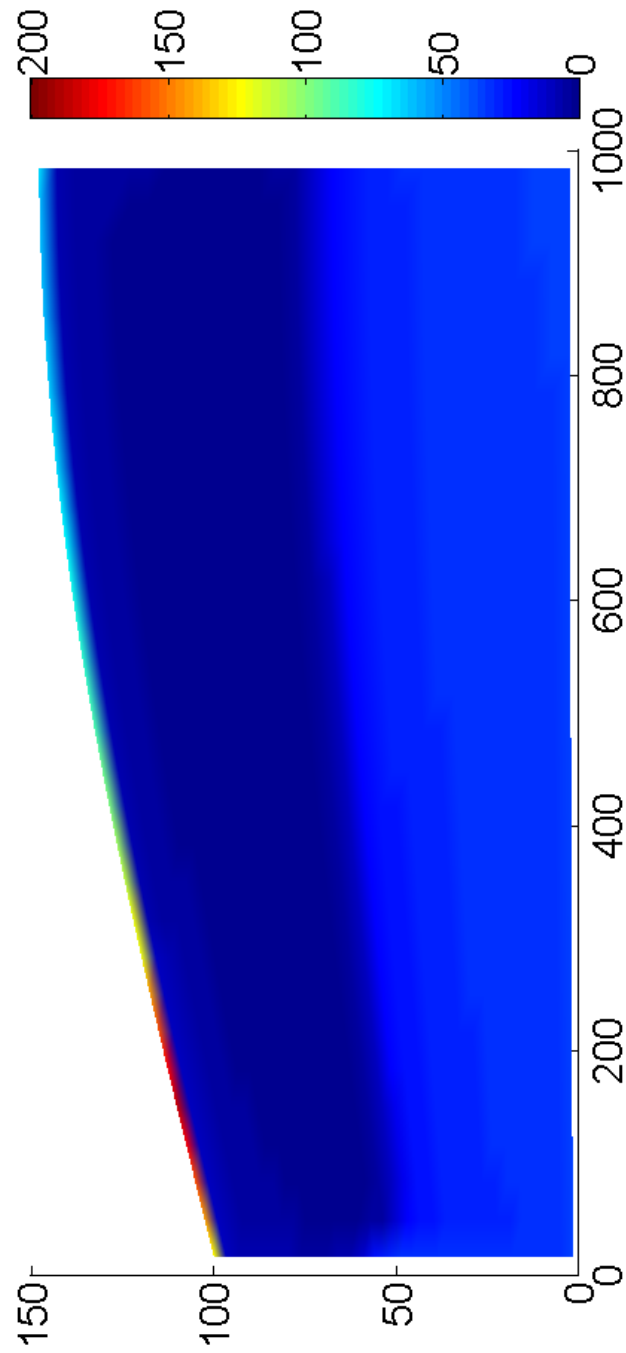
Figure 5.17: The above shows the bacteria profile with rain wetting using $f_2(\Theta)$ after a twenty-four hour period. The rain was simulated from hours one to nineteen.
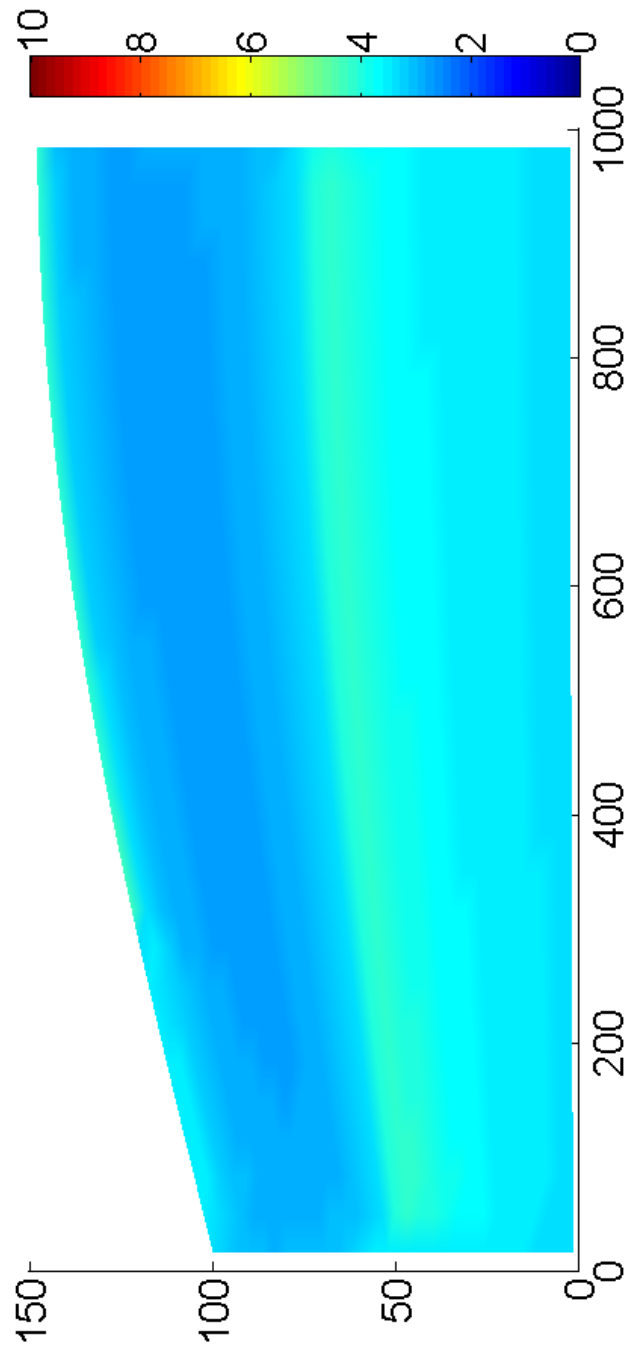
Figure 5.18: This shows the nutrient profile of the beach after a total twenty-four hour period and with rain wetting from hours one to nineteen. $f_2(\Theta)$ was used for this simulation.

most growth. Note that even though the moisture seeps into the domain as shown in Figure 5.4, the bacteria remain mostly on the top of the beach. This can be caused, in part, to the choice for ξ_1 which controls how much the moisture flux influences the movement of bacteria through the sand.

Figure 5.20 shows the result of the simulation when using $f_4(\Theta)$. Although there is an increase in the bacterial counts, it is not as prominent as with the three previous simulations. Another difference is the location of bacterial growth. With this moisture preference, there is a band of growth about half way down the sand, identical to what was seen in the previous section, and there is preference for growing just above the area where the wave dampening occurs. Note that there is no scale change for this model from the previous section when there was no rain dampening simulated. The lack of a spike in bacterial growth on the surface of the beach indicates that $f_4(\Theta)$ is not a good model for bacterial growth. Additionally, studies suggest that bacteria prefer to grow in sand where there is some wave action [37, 38], and this is an important consideration when understanding this model. The fact that $f_4(\Theta)$ does not show a preference for bacterial growth where there is wave dampening further indicates that this model is not appropriate.

As with the previous section, the amount of bacteria and nutrient fluxed through the domain boundaries was tracked throughout the simulation and the results of for $f_2(\Theta)$ are shown in Figures 5.21 and 5.22. The fluxes through the bottom as well as the right and left sides were essentially identical to the respective fluxes in Figures 5.14 and 5.15. As with those plots, the bacteria and nutrient fluxes through the right, left, and bottom boundary are plotted time step for time step and the fluxes through the top boundary were averaged every hour and then plotted.

As a result of the rain dampening, there is a greater amount of nutrient and bacteria fluxed through the top border during the rain event. At no one point did the top boundary flux in more than six CFU's of bacteria per 100 cm^3 or one μmol

Figure 5.19: The above figure shows the bacteria profile with rain wetting using $f_3(\Theta)$. This profile is the result of a total twenty-four hour simulated period with moisture added to the top boundary from hours one to nineteen.
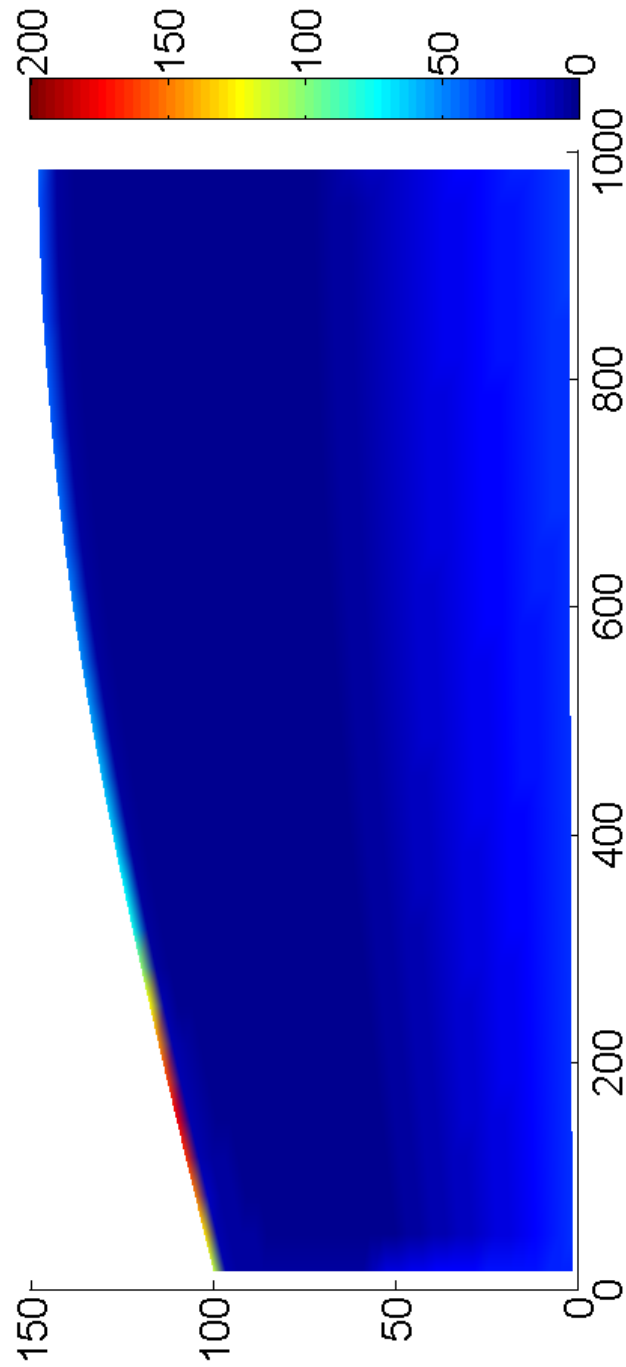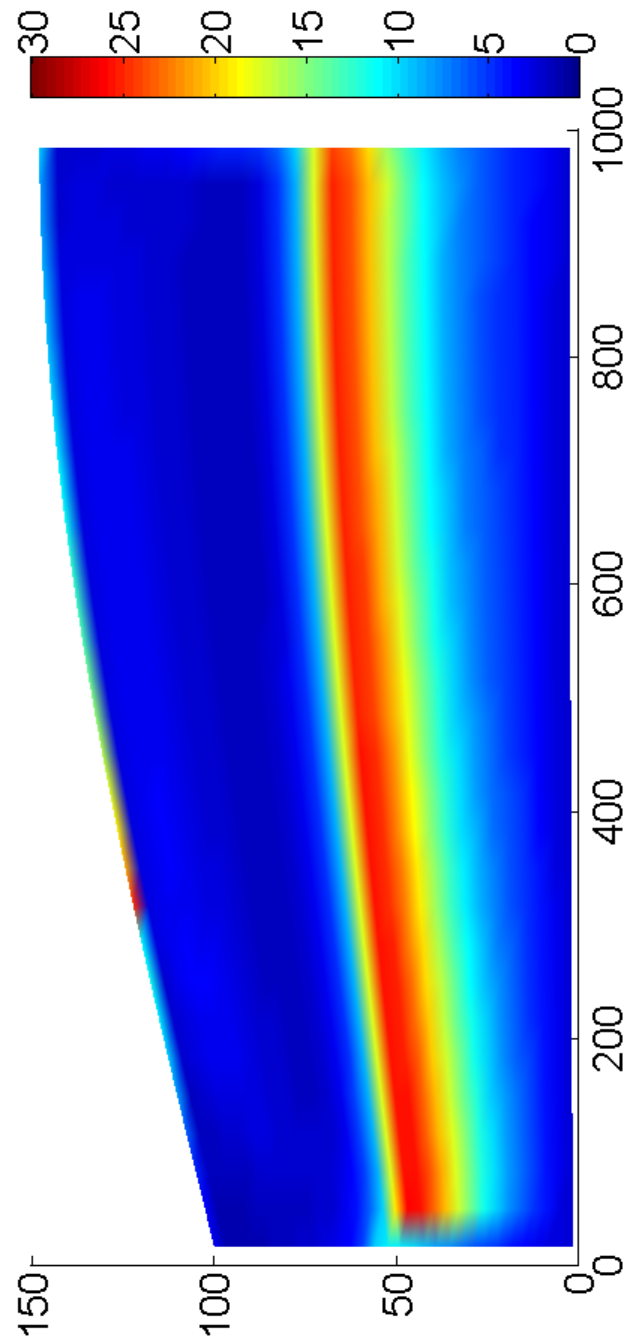
Figure 5.20: The above figure shows the bacteria profile with rain wetting using $f_4(\Theta)$. This profile is the result of a total twenty-four hour simulated period. From hours one to nineteen, moisture is added to the top boundary.

of nutrient per 100 cm^3. In reality, when it rains, there is more bacteria and nutrient that is fluxed into the system than what is simulated here. Similarly to the bacteria and nutrient flux tracking in the previous section, the Dirichlet boundary conditions related to the moisture are adding bacteria and nutrient when there is dampening, but when the top boundary is made to have a moisture value of 0.1, some of the bacteria and nutrient are fluxed back out of the domain. Still, our simulation shows that the rain dampening provides more favorable conditions for bacterial growth and our simulations show bacteria being sourced from the sand. Monitoring bacterial growth solely in the body of water may not be sufficient in understanding the health of a beach.

Figure 5.21: The above shows the bacteria fluxed through the domain boundaries as a result of simulating a twenty-four hour period using $f_2(\Theta)$ with constant wave wetting and rain wetting from hours one to nineteen. Although difficult to distinguish in the figure, the values for the left boundary closely match those of the right boundary.

The figures presented here were chosen so that the scale provided could show the

areas of highest bacterial growth as well as allow for estimation of what the final bacteria counts are in those areas of high growth. If the scale is lowered, it can be more easily seen that bacteria grow along the entire top of the beach during a rain dampening event. For the profiles of $f_1(\Theta)$, $f_2(\Theta)$, and $f_3(\Theta)$ presented in this section, some bacterial growth can be seen along the entire surface of the beach, but it is not as much growth as what is seen closer to the body of water.
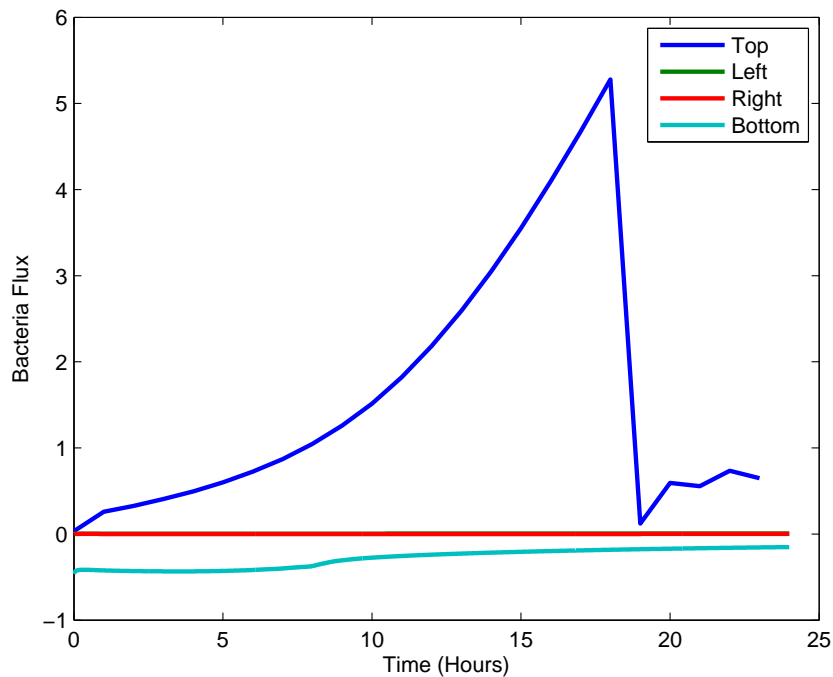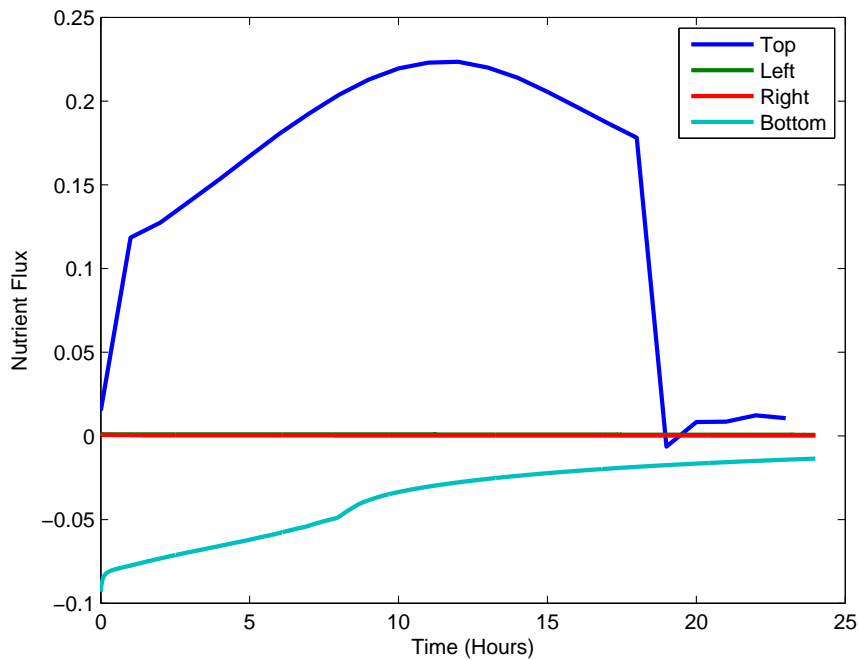

Figure 5.22: The above shows the nutrient fluxed through the domain boundaries as a result of simulating a twenty-four hour period using $f_2(\Theta)$ with constant wave wetting and rain wetting from hours one to nineteen. Although difficult to distinguish in the figure, the values for the left boundary closely match those of the right boundary.

For all simulations there is not a great difference between where the immobile and mobile bacteria prefer to grow. The only difference is that there is slightly more mobile bacteria that grow where moisture is being fluxed in via the simulated rain and wave wetting. This can be partially accounted for in that it is only mobile bacteria that are being fluxed in or out of the system, but it is also accounted for by the fact that bacterial growth occurs where there is moisture and all bacteria start as mobile

bacteria.

Recent research shows that rain events correlate to an increase in bacterial growth, but that within a certain time frame, the bacterial counts return to pre-rain levels without totally diminishing [38]. Our model does not include any factor that could inhibit growth as long as there is wave dampening because the death rate is treated as a constant. Expanding upon the assumptions of this model and including new assumptions about other factors impacting bacterial growth could help us understand the fluctuation in growth around rain events.

5.2.4 Temperature Considerations

It is very difficult to properly account for all types of weather and their affect on beaches. Although the results of the presented simulations show that there can be growth as deep as 100 centimeters into the beach, data from the literature suggests this is not always the case [37]. One reason for this could be that the temperature of the sand decreases with depth. The sand deeper in the beach is colder than the sand on the surface. Since rain would cause the temperature of the sand to become lower than it would be on a sunny day, we simply considered the case where there is no rain wetting. An assumed temperature profile of the beach is shown in Figure 5.23.

In order to get this profile, it was assumed that the top of the beach had a temperature of 30° Celcius and that the temperature decreased by 0.2° for every centimeter of depth until a temperature of 12° was reached. At that point it was assumed that the temperature had reached an equilibrium and all sand below maintained a temperature of 12° [37, 40]. Then, a scalar was multiplied by μ according to the temperature. *E. coli* prefer to grow at approximately 37° so a normal distribution centered around thirty-seven was created to try to closely match the shape of the function used in previous studies [18]. This resulted in the growth simply being scaled by some positive number no greater than one. Naturally, the bacterial growth was not as great,
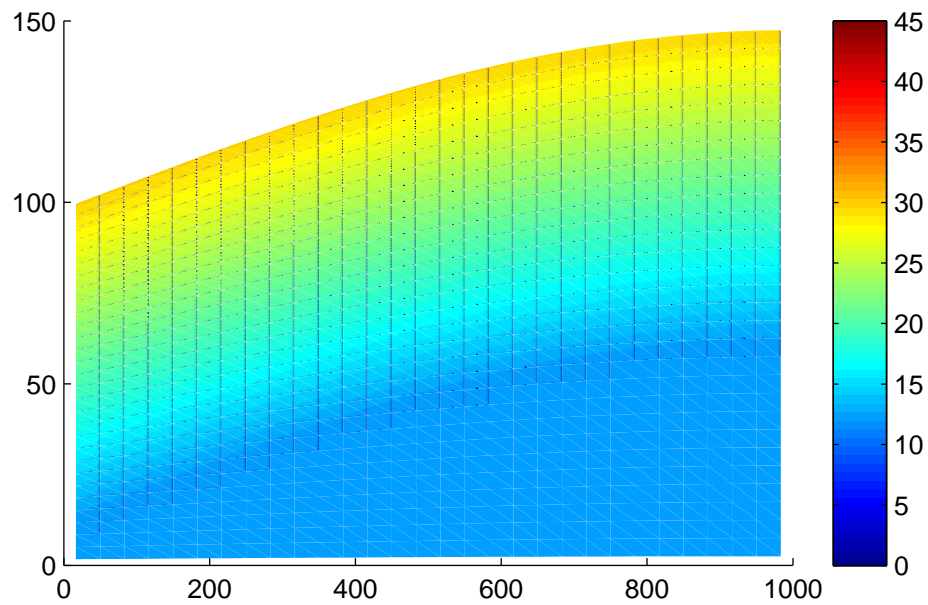
Figure 5.23: The above figure shows the temperature profile of the beach when temperature is modeled as a function of depth.

but after twenty-four hours, the bacteria counts were actually less than those given by the initial conditions. The closer the temperature is to the preferred value of $37°$, the more growth there will be. The same parameter values as before were used and the simulation was run using $f_2(\Theta)$ and only wave wetting. The results are shown in Figure 5.24.

A similar idea was used in previous studies of bacterial growth and temperature, but the function of growth with respect to temperature proved to be difficult to implement for these simulations [18]. Currently it is known that bacteria have certain temperature ranges that provide optimal growth, but the relationship between the temperature and growth rate is not as simple as using a normal distribution to model temperature dependence. A better understanding of the relationships between temperature, moisture, nutrient level, and other factors is needed in order to properly implement temperature in this model.

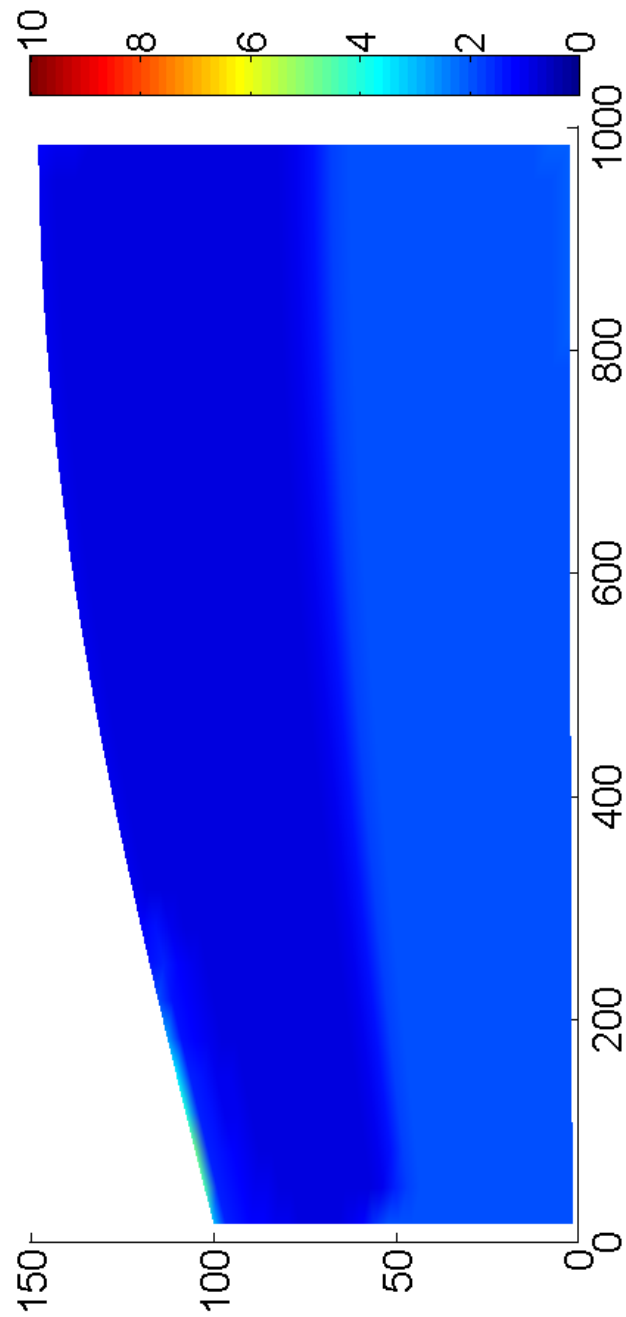Figure 5.24: The above figure is of the total bacteria profile and shows results of simulations using $f_2(\Theta)$ after twenty-four hours when temperature is considered as a factor in bacterial growth.

6   Discussion

Given the fact that Richards Equation is meant to model moisture movement solely in unsaturated soil, it is difficult to flood the entire domain and still have biologically accurate solutions to the equation. As a topic of further study, it is important to consider changing the algorithm so that the domain can have both saturated and unsaturated cells. The saturated cells could be treated one way by the algorithm and unsaturated cells can still be treated by algorithm presented. This expansion of the model would be incorporating two different models for moisture movement, each with changing domains, but it would also provide a more accurate model and a way to study the effect of groundwater moving through the bottom of the domain.

The treatment of the rain and wave modeling would be made more accurate if there was added pressure when the top boundary is made wet. This would be a component in the modeling of a saturated domain. Additionally, the values of ξ_1 and ξ_2 are probably much closer to one than the values used in the simulations. These values can be better treated if there is a simulation involving both saturated and unsaturated portions of the domain.

Adding the y component, the third dimension, would be a practical extension of this model as well. For this paper, it was assumed that the cross-section of the beach was representative of the entire beach in the third dimension. Adding the third dimension would allow for different considerations on the boundaries.

It would also be useful to utilize a mesh refinement system for this model. This would allow the domain mesh to include more cells in areas where there is high of flux between cells; although it could make modeling waves more difficult. Refining the mesh where needed could give more accurate results as well as less accumulated interpolation error.

The moisture, nutrient, and bacterial dynamics simulated show that bacteria prob-

ably prefer a relative moisture level greater than 0.5. The $f_1(\Theta)$, $f_2(\Theta)$, and $f_3(\Theta)$ seemed to be better candidates for modeling bacterial growth than $f_4(\Theta)$. The spikes in growth and preference for growing in sand affected by wave wetting was seen in all but $f_4(\Theta)$, and these are important patterns that have been verified in the literature [37, 38]. It is impossible to state whether any of the three remaining candidates provide a better model than the other two given that the results are so close. While there is growth below fifty centimeters in every simulation, changing the assumptions to account for temperature and differences in sand grain porosity below the surface of the beach could help the model align with the published research stating that there is not as much, if any, bacterial growth as deep as fifty centimeters into the beach [37]. Although temperature was considered as a factor impacting growth, a full implementation of temperature with the model is a topic of further study.

For the bacteria and nutrient models, sufficient data could not be found. Although the parameters related to moisture movement are documented, most of the parameters related to bacterial growth were estimated based on what information could be found in the literature. In many cases, the parameters were chosen based on many trials run with different parameter values and then comparing the results of those trials to general patterns of bacterial growth that have been discussed in the literature [2, 20, 24, 34, 37, 38].

It would also be valuable to look at modeling these scenarios over a longer period of time. Rain events are correlated with spikes in the number of bacteria in sand, and then the bacterial counts return to some normal level after the rain has passed and it would be beneficial to see if this can also be simulated [38]. With our current model, there would not be any decrease in the bacterial population after a rain event. This is because there are other factors at play besides basic nutrients and moisture which are not represented. Predation, competition, and sunlight often lead to a decrease in bacterial counts in water versus the sand [37, 38, 39]. Changing the death rate to be a

function of sunlight, among other factors, could make the model more accurate if we want to simulate what happens to the bacteria population during longer periods of time. Another possible change could be making the growth rate a function of factors that limit bacterial growth as well as moisture and nutrient. The model presented accounts for the basic need for nutrients and water, but more information is needed to model the complexity of bacterial survival. In order to better predict the long term growth of bacteria on beaches, we need a more thorough understanding of these relationships.

REFERENCES

[1] Assouline, S. & Tartakovsky, D.M. (2001) *Unsaturated Hydraulic Conductivity Function Based on a Soil Fragmentation Process.* Water Resour. Res. **37** pp. 1309-1312.

[2] Auset, M., Keller, A.A., Brissaud, F., & Lazarova, V. (2005) *Intermittent Filtration of Bacteria and Colloids in Porous Media.* Water Resour. Res. **41** W09408.

[3] Bear, J. & Cheng, A.. (2010) *Modeling Groundwater Flow and Contaminant Transport.* Springer.

[4] Bell, A. (2013). Lecture notes. *Math 631/632: Modern Algebra.* Personal Collection of A. Bell, University of Wisconsin-Milwaukee, Milwaukee, WI.

[5] Bright, T.M., Hathaway, J.M., Hunt III, W.F., de los Reyes III, F.L., & Burchell II, M.R. (2010) *Impact of Storm-Water Runoff on Clogging and Fecal Bacteria Reduction in Sand Columns.* J. Environ. Eng-ASCE. **136** pp. 1435-1441.

[6] Bruckner, A., Catenacci, J. & Schroeder, M. (2011) *Analysis and simulation of bacterial contamination on an urban beach at Lake Michigan.* Paper presented at the National Conference of Undergraduate Research, Ogden, Utah, March 29-31, 2012.

[7] Causon, D.M., Mingham, C.G., & Qian, L. (2011) *Introductory Finite Volume Methods for PDEs.* Ventus Publishing ApS.

[8] Ciarlet, G. & Lions, J.L. (2000) *Handbook on Numerical Analysis.* **7** North-Holland.

[9] Craft, T.J. *Review of Basic Finite Volume Methods* [PDF slides]. Retrieved from: `cdf.mace.manchester.ac.uk/twiki/pub/Main/TimCraftNotes_All_Access /ms4-fvreviews.pdf`.

[10] Dong, H., Rothmel, R., Onstott, T.C., Fuller, M.E., DeFlaun, M.F., Streger, S.H., Dunlap, R. & Fletcher, M. (2002) *Simultaneous Transport of Two Bacterial Straing in Intact Cores from Oyster, Virginia: Biological Effects and Numerical Modeling.* Appl. Environ. Microbiol. **68** pp. 2120-2132.

[11] Eymard, R., Gutnic, M. & Hilhorst, D. (1999) *The Finite Volume Method for Richards Equation.* Computat Geosci. **3** pp. 259-294.

[12] Eliassi, M. & Glass, R.J. (2001) *On the Continuum-Scale Modeling of Gravity-Driven Finges in Unsaturated Porous Media: The Inadequacy of the Richards Equation with Standard Monotonic Constitutive Relations and Hysteretic Equations of State.* Water Resour. Res. **37** pp. 2019-2035.

[13] Forsyth, P.A., & Sammon, P.H. (1988) *Quadratic Convergence for Cell-Centered Grids.* Appl. Num. Math. **4** pp. 377-394.

[14] Fujikawa, H., Kai, A. & Morozumi, S. (2003) *A New Logistic Model for Bacterial Growth.* J. Food Hyg. Soc. Japan **44** pp. 155-160.

[15] Ge, Z. & Frick, W.E. (2009) *Time-Frequency Analysis of Beach Bacteria Variations and its Implication for Recreational Water Quality Modeling.* Environ. Sci. Technol. **43** pp. 1128-1133.

[16] Igel, H. *Finite Volumes* [slides]. Retrieved from Lecture Notes: `www.geophysik.uni-muenchen.de/~igel/downloads/nmgiifv.pdf`.

[17] Lauko, I. (2013). Lecture on Numerical Solutions of PDE's. Personal Collection of I. Lauko, University of Wisconsin-Milwaukee, Milwaukee, WI.

[18] Leahy, M.J., Davidson, M.R., & Schwarz, M.P. (2005) *A Model for Heap Bioleaching of Calcocite with Heat Balance: Bacterial Temperature Dependence.* Miner. Eng. **18** pp. 1239-1252.

[19] Leij, F.J., Alves, W.J., van Genuchten, M.Th. & Williams, J.R. (1996) *The UNSODA Unsaturated Soil Hydraulic Database.* EPA/600/R-96/095, National Risk

Management Laboratory, Office of Research and Development, U.S. Environmental Protection Agency, Cincinnati, OH.

[20] Louge, M.Y., Valance, A., Ould el-Moctar, A., Xu, J., Hay, A.G., & Richer, R. (2013) *Temperature and Humidity Within a Mobile Barchan Sand Dune, Implications for Microbial Survival.* J. Geophys. Res. **118** pp. 2392-2405.

[21] McCallum, W.G., Hughes-Hallett, D., Gleason, A.M., *et. al.* (2002) *Multivariable Calculus: Third Edition.* John Wiley & Sons, Inc.

[22] Misiats, O. & Lipnikov, K. (2012) *Second-Order Accurate Monotone Finite Volume Scheme for Richards' Equation.* J. Comput. Phys. **239** pp. 123-137.

[23] Mostafa, M. & Van Geel, P.J. (2007) *Conceptual Models and Simulations for Biological Clogging in Unsaturated Soils.* Vadose Zone J. **6** pp. 175-185.

[24] Murphy, E.M. & Ginn, T.R. (2000) *Modeling microbial processes in porous media.* Hydrogeol. J. **8** pp. 142-158.

[25] Newcombe, C.L. (1935) *Certain Environmental Factors of a Sand Beach in the St Andrews Region, New Brunswick, With a Preliminary Designation of the Intertidal Communities.* J. Ecol. pp.334-355.

[26] Nimmo, J.R. & Landa, E.R. (2005) *The Soil Physics Contributions of Edgar Buckingham.* Soil Sci. Soc. Am. J. **69** pp. 328-342.

[27] Rajkai, K., Kabos, S., & van Genuchten, M.Th. (2004) *Estimating the Water Retention Curve from Soil Properties: Comparison of Linear, Nonlinear, and Concomitant Variable Methods.* Soil Til. Res. **79** pp. 145-152.

[28] Rosenzweig, R., Shavit, U. & Furman, A. (2009) *The Influence of Biofilm Spatial Distribution Scenarios on Hydraulic Conductivity of Unsaturated Soils.* Vadose Zone J. **8** pp. 1080-1084.

[29] Schaap, M.G. (1999) *Rosetta: A Computer Program for Estimating Soil Hydraulic Parameters with Hierarchical Pedotransfer Functions.* http://cals.arizona.edu/research/rosetta/.

[30] Stanescu, D. & Chen-Charpentier, B.M. (2009) *Random Coefficient Differential Equation Models for Bacterial Growth.* Math. Comput. Model. **50** pp. 885-895.

[31] Szymkiewicz, A. (2013) *Modelling Water Flow in Unsaturated Porous Media.* Springer.

[32] Thullner, M., Van Cappellen, P. & Pegnier, P. (2005) *Modeling the Impact of Microbial Activity on Redox Dynamics in Porous Media.* Geochim. Cosmochim. Ac. **69** pp. 5005-5019.

[33] Tindall, J.A. & Kunkel, J.R. (1998) *Unsaturated Zone Hydrology for Scientists and Engineers.* Pearson Education.

[34] Tufenkji, N. (2007) *Modeling Microbial Transport in Porous Media: Traditional Approaches and Recent Developments.* Adv. Water Resour. **30** pp 1455-1469.

[35] van Genuchten, M.Th. (1980) *A Closed-Form Equation for Predicting the Hydraulic Conductivity of Unsaturated Soils.* Soil. Sci. Soc. **44** pp. 892-898.

[36] van Genuchten, M.Th. & Nielsen, D.R. (1985) *On Describing and Predicting the Hydraulic Conductivity of Unsaturated Soils.* Ann. Geophys. pp. 615-628.

[37] Wheeler Alm, E., Burke, J. & Spain, A. (2003) *Fecal Indicator Bacteria are Abundant in Wet Sand at Freshwater Beaches.* Water Res. **37** pp. 3978-3982.

[38] Whitman, R. & Nevers, M. (2003) *Foreshore Sand as a Source of Escherichia coli in Nearshore Water of a Lake Michigan Beach.* Appl. Environ. Microbiol. **69** pp. 5555-5562.

[39] Whitman, R., Nevers, M., Korinek, G. & Byappanahalli, M.N. (2004) *Solar and Temporal Effects on Escherichia coli Concentration at a Lake Michigan Swimming Beach.* Appl. Environ. Microbiol. **70** pp. 4276-4285.

[40] Wuest, S.B. (2012) *An Array for Measuring Detailed Soil Temperature Profiles.* Soil. Sci. Soc. Am. J. **77** 427-431.

[41] Yarwood, R.R., Rockhold, M.L., Niemet, M.R., Selker, J.S. & Bottomley, P.J. (2006). *Impact of Microbial Growth on Water Flow and Solute Transport in Unsaturated Porous Media.* Water Resour. Res. **42** W10405.

[42] Yates, S.R., van Genuchten, M.Th., Warrick, A.W. & Leij, F.J. (1992) *Analysis of Measured, Predicted, and Estimated Hydraulic Conductivity Using the RETC Computer Program.* Soil Sci. Soc. Am. J. **56** pp. 347-354.